Published in final edited form as:
Neuroscience. 2009 August 4; 162(1): 128–147. doi:10.1016/j.neuroscience.2009.04.054.

PARATHYROID HORMONE 2 RECEPTOR AND ITS ENDOGENOUS LIGAND TIP39 ARE CONCENTRATED IN ENDOCRINE, VISCEROSENSORY AND AUDITORY BRAIN REGIONS IN MACAQUE AND HUMAN

Attila G. Bagó[1,2,§], **Eugene Dimitrov**[3,§], **Richard Saunders**[4], **László Seress**[5], **Miklós Palkovits**[1], **Ted B. Usdin**[3,*], and **Arpád Dobolyi**[1,*]

1 *Neuromorphological and Neuroendocrine Research Laboratory, Department of Anatomy, Histology and Embryology, HAS - Semmelweis University, Budapest*

2 *National Institute of Neurosurgery, Budapest, Hungary*

3 *Section on Fundamental Neuroscience, National Institute of Mental Health, Bethesda, Maryland, USA*

4 *Laboratory of Neuropsychology, National Institute of Mental Health, Bethesda, Maryland, USA*

5 *Central Electron Microscopic Laboratory, University of Pécs, Pécs, Hungary. Section Editor: Dr. M. Witter*

Abstract

Parathyroid hormone receptor 2 (PTH2R) and its ligand, tuberoinfundibular peptide of 39 residues (TIP39) constitute a neuromodulator system implicated in endocrine and nociceptive regulations. We now describe the presence and distribution of the PTH2R and TIP39 in the brain of primates using a range of tissues and ages from macaque and human brain. *In situ* hybridization histochemistry of TIP39 mRNA, studied in young macaque brain, due to its possible decline beyond late postnatal ages, was present only in the thalamic subparafascicular area and the pontine medial paralemniscal nucleus. In contrast *in situ* hybridization histochemistry in macaque identified high levels of PTH2R expression in the central amygdaloid nucleus, medial preoptic area, hypothalamic paraventricular and periventricular nuclei, medial geniculate, and the pontine tegmentum. PTH2R mRNA was also detected in several human brain areas by RT-PCR. The distribution of PTH2R-immunoreactive fibers in human, determined by immunocytochemistry, was similar to that in rodents including dense fiber networks in the medial preoptic area, hypothalamic paraventricular, periventricular and infundibular (arcuate) nuclei, lateral hypothalamic area, median eminence, thalamic paraventricular nucleus, periaqueductal gray, lateral parabrachial nucleus, nucleus of the solitary tract, sensory trigeminal nuclei, medullary dorsal reticular nucleus, and dorsal horn of the spinal cord. Co-localization suggested that PTH2R fibers are glutamatergic, and that TIP39 may directly influence hypophysiotropic somatostatin containing and indirectly influence corticotropin releasing-hormone containing neurons. The results demonstrate that TIP39 and the PTH2R are expressed in the brain

*Authors for correspondence, proofs and reprint requests: Dr. Ted B. Usdin, Section on Fundamental Neuroscience, NIMH, Bethesda MD 20892-3728, Bldg 35/Rm1B-215. {35 Convent Dr MSC 3728 (U.S. mail)}, Tel.: 301-402-6976; fax.: +1-301-435-5465, e-mail address: E-mail: usdint@mail.nih.gov. Dr. Arpád Dobolyi, Laboratory of Neuromorphology, Department of Anatomy, Histology and Embryology, Semmelweis University, Budapest Hungary H-1094, Tüzoltó u. 58. Tel.: +36-1-215-6920/3634, fax.: +36-1-218-1612, e-mail address: E-mail: dobolyi@ana.sote.hu.
§These authors contributed equally to this work.

of primates in locations that suggest involvement in regulation of fear, anxiety, reproductive behaviors, release of pituitary hormones, and nociception.

Keywords

tuberoinfundibular peptide; neuroendocrine modulator; primate hypothalamus; subparafascicular area; medial paralemniscal nucleus; in situ hybridization in monkey brain

---

Tuberoinfundibular peptide of 39 residues (TIP39) and the parathyroid hormone 2 receptor (PTH2R) constitute a peptide/receptor neuromodulator system. The function of this system is being investigated in rodents. Data suggest the system modulates neuroendocrine, anxiety-related and nociceptive functions. Comparison of the anatomical distribution of the system in primates and rodents is important for extrapolation of experimental results obtained in rodents to humans.

The PTH2R was identified on the basis of its sequence homology to other polypeptide-recognizing receptors (Usdin et al., 1995). It is a seven transmembrane domain receptor, which belongs to the type II (or family B) class of G-protein-coupled receptors (Harmar, 2001, Usdin et al., 2002). The human PTH2R has about 84% amino acid sequence identity with the rodent PTH2R and about 50% with the human parathyroid hormone 1 receptor (PTH1R). Tuberoinfundibular peptide of 39 residues (TIP39) was purified from bovine hypothalamus on the basis of its selective activation of the PTH2R (Usdin et al., 1999b). Mouse and rat TIP39 sequences, as well as human and bovine TIP39 sequences, are identical while amino acids differ at 4 positions between rodent and human TIP39 sequences (Dobolyi et al., 2002, John et al., 2002, Usdin et al., 2003). Rodent TIP39 sequences share only 6, and 4 amino acid residues with parathyroid hormone (PTH), and parathyroid hormone-related peptide (PTHrP), respectively, while the corresponding numbers of amino acid similarities for human peptides are 8 and 5. The PTH1R is activated with subnanomolar potency by PTH and PTHrP, and both peptides are thought to be its physiological ligands. PTH is released from the parathyroid glands and has a critical role in calcium metabolism, whereas PTHrP is produced locally and is involved in the development and remodeling of many tissues, especially the skeleton (Kronenberg et al., 1998). In contrast, TIP39 has no significant effect on the PTH1R (Hoare et al., 2000). The human PTH2R is potently activated by both PTH and TIP39 (Usdin et al., 1999b). TIP39 potency on the rat PTH2R is similar to that on the human receptor, whereas PTH is several thousand-fold less potent and produces only 40% of TIP39's maximal effect (Usdin et al., 1999b). PTHrP does not activate the rat or human PTH2R (Hoare and Usdin, 2001). Thus, there is strong pharmacological evidence that TIP39 is an endogenous ligand for the PTH2R (Usdin et al., 2000).

The PTH2R is most abundant in the brain (Usdin et al., 1995) which contains little if any PTH (Usdin, 1997). The localization of PTH2R-expressing cell bodies as well as nerve fibers and terminals has been described in detail in rat (Wang et al., 2000) and mouse (Faber et al., 2007). Neuronal cell bodies are in general difficult to detect using antibody labeling but their distribution has been demonstrated using *in situ* hybridization histochemistry (Wang et al., 2000, Faber et al., 2007) and labeling of beta-galactosidase in knock-in mice with beta-galactosidase driven by the PTH2R promoter (Faber et al., 2007). The PTH2R is expressed in the cerebral cortex, the caudate nucleus, the lateral septal nucleus, the bed nucleus of the stria terminalis, the central and medial amygdaloid nuclei, the medial preoptic area, the hypothalamic periventricular, paraventricular and arcuate nuclei, midline and intralaminar thalamic nuclei, the medial geniculate body, the pretectal and ventral tegmental areas, the superior colliculus, the pontine tegmentum, the nucleus of the solitary tract, and the cerebellar cortex. In general, these regions contain a matching density of PTH2R-immunoreactive (-ir)

fibers, which are also abundant in the median eminence, the periaqueductal gray, the lateral parabrachial nucleus, the sensory trigeminal nuclei, and lamina II of the spinal cord dorsal horn (Wang et al., 2000, Faber et al., 2007). Moreover, in rodents the distribution of TIP39-ir fibers and fiber terminals correlates almost perfectly with the brain areas containing PTH2Rs (Dobolyi et al., 2003b, Faber et al., 2007). Furthermore, even the subregional distribution of TIP39- and PTH2R-immunoreactive fibers in these regions showed remarkable similarities in rats (Dobolyi et al., 2006a) as well as in mice (Faber et al., 2007), providing anatomical evidence that TIP39 acts on the PTH2R neurons.

TIP39 neurons restricted to two discrete brain regions give rise to the widely distributed TIP39-ir fibers in both rats and mice (Dobolyi et al., 2003b, Faber et al., 2007). One of them is the subparafascicular area (Wang et al., 2006b), which extends from a medial part in the periventricular gray of the thalamus postero-laterally to the medial geniculate body. The other one is the medial paralemniscal nucleus at the midbrain-pons junction (Varga et al., 2008). It has been established by their disappearance following lesions, as well as by anterograde tracer techniques, that TIP39-ir fibers in limbic and endocrine regions originate in the subparafascicular area while auditory, and nociceptive-viscerosensory regions including the lateral parabrachial nucleus and the spinal cord receive TIP39-ir projections from the medial paralemniscal nucleus (Dobolyi et al., 2003a, Wang et al., 2006c).

Initial functional studies implicate TIP39 in the modulation of some aspects of spinal nociceptive signaling (Dobolyi et al., 2002) and in the modulation of an affective component of nociception (LaBuda and Usdin, 2004). Furthermore, c-Fos activation in brain areas expressing TIP39, suggests that TIP39 neurons may be involved in central regulation of reproduction (Lin et al., 1998, Li et al., 1999, Coolen et al., 2004). Specifically, c-Fos activation has been demonstrated in subparafascicular TIP39 neurons following male sexual behavior (Wang et al., 2006a). An experiment using positron emission tomography to measure increases in regional cerebral blood flow suggests that the subparafascicular area is also activated during human male ejaculation (Holstege et al., 2003). TIP39 has also been suggested to affect the neuroendocrine system. It may regulate the release of pituitary hormones (Ward et al., 2001, Sugimura et al., 2003, Usdin et al., 2003) and is potentially involved in the audiogenic stress response (Palkovits et al., 2004). In addition, intra-cerebroventricular injection of TIP39 resulted in anxiolytic- and antidepressant-like effects (LaBuda et al., 2004). Furthermore, a very recent study demonstrated increased fear and stress-related anxiety-like behavior in mice lacking TIP39 (Fegley et al., 2008).

There is extremely limited information on TIP39 and the PTH2R in primates. A human PTH2R cDNA has been cloned and both sequences have been identified in the human genome. TIP39 was found in total brain cDNA by RT-PCR and in a preliminary study we reported evidence for the expression of the PTH2R in combined brainstem samples using RT-PCR (Bago et al., 2008). We have now investigated the anatomical expression patterns of TIP39 and the PTH2R in macaque and human brain so that a comparison can be made to the comprehensive mapping that has been performed in rodents. There is a dramatic decline in TIP39 expression during postnatal development in the rat brain (Dobolyi et al., 2006b), so, we used the brain of a 3 day-old macaque to identify the location of TIP39 neurons, by *in situ* hybridization histochemistry. We also mapped the distribution of PTH2R mRNA in a representative set of areas in this brain, because PTH2R expression did not change during postnatal development in the rat (Dobolyi et al., 2006b). In material from an adult macaque we investigated whether PTH2R neurons are glutamatergic by performing double labeling with antibodies to the PTH2R and vesicular glutamate transporter 2. We confirmed that humans have a similar distribution of PTH2R synthesis by mapping the expression of the PTH2R in several different brain regions by RT-PCR in adult. We used immunohistochemistry to examine the distribution of PTH2R-immunoreactive fibers in material from both young and old humans in a number of brain

regions selected to provide comparison with rodent data. Since TIP39 has been suggested to alter plasma growth hormone and corticosterone levels (Ward et al., 2001, Usdin et al., 2003), we also investigated the anatomical relationship between the PTH2R and hypophysiotropic somatostatin-, and corticotropin-releasing hormone (CRH)-containing neurons.

EXPERIMENTAL PROCEDURES

Human tissue

Human brain samples were collected in accordance with the Ethical Rules for Using Human Tissues for Medical Research in Hungary (HM 34/1999) and the Code of Ethics of the World Medical Association (Declaration of Helsinki). Tissue samples were taken during brain autopsy at the Department of Forensic Medicine of Semmelweis University in the framework of the Human Brain Tissue Bank, Budapest, or at the Department of Pathology of the University of Pécs, as approved by institutional ethics committees of the Semmelweis University or the University of Pécs. Prior written informed consent was obtained from the next of kin, which included the request to consult the medical chart and to conduct neurochemical analyses. The study reported in the manuscript was performed according to animal care protocols approved by the Committee of Science and Research Ethics, Semmelweis University (TUKEB 34-1/2002). The medical history of the subjects was obtained from medical or clinical records, interviews with family members and relatives, as well as from pathological and neuropathological reports. All personal identifiers had been removed and samples coded before the analyses of tissue.

Brains were removed from the skull with a post-mortem delay of 2–6 h. For microdissection, the brains were cut into 5 large parts (cerebral lobes, diencephalon, brainstem, cerebellum), and frozen immediately at −80 °C. For immunocytochemistry, brains were cut into 5–10 mm thick coronal slices and immersion fixed in 4% paraformaldehyde in 0.1 M phosphate buffer (PB) for 6–10 days. Then, the slices were postfixed in the same solution with addition of 15% saturated picric acid.

Microdissection of human brain tissue

Brain nuclei and areas including the frontal cortex, hippocampus, septum, caudate nucleus, amygdala, ventral thalamus, mediodorsal thalamic nucleus, pulvinar, lateral and medial geniculate bodies, subthalamic nucleus, medial hypothalamus, pretectal area, substantia nigra, ventral tegmental area, pontine nuclei, tegmentum and reticular formation, ventrolateral medulla, dorsal vagal complex, inferior olive, spinal trigeminal nucleus, and cerebellar cortex were individually microdissected from the brains of an 89 year old woman and a 56 year old man using the micropunch technique (Palkovits, 1973, Palkovits et al., 2008) guided by human brain atlases (Paxinos and Huang, 1995, Mai et al., 1997). Briefly, the large parts of the frozen brains were cut into 1.0–1.5 mm thick coronal sections by an electric slicer at about −5–10 °C, and individual brain regions and nuclei were removed from the slides by special punch needles with an inside diameter of 1.0–3.5 mm visualized using either a head magnifier, or a stereomicroscope. The slices were kept on dry-ice during the whole procedure. The microdissected samples were collected in 2.0 mm airtight plastic (Eppendorf) tubes and stored at −80 °C until further use.

RT-PCR of the PTH2R from human

Total mRNA was isolated using Trizol^{R} Reagent (Invitrogen, Carlsbad, CA) from 50–100 mg of brain tissue according to the manufacturer's instructions. The degradation of RNA was assessed by running the purified RNAs on denaturing formaldehyde gels. Samples, in which the amount of 28S rRNS was at least equal to that of 18S rRNA were processed further for

RT-PCR. After diluting total RNA to 2 μg/μl, RNA was treated with Amplification Grade DNase I (Invitrogen) and cDNA was synthesized with a Superscript II reverse transcriptase kit (Invitrogen) according to the manufacturer's instructions. After 10-fold dilution, 2.5 μl of the resulting cDNA was used as template in PCR reactions. The primer pair for PTH2R was 5′-CAATTGCTTGGCTGTAGCTTT-3′ and 5′-ACAAAATCAATTTGCAGACACAA-3′ resulting in a PCR product of 440 bp that corresponds to bp 2162–2601 of the human PTH2R (GeneBank accession number NM_005048). The PCR product using this PTH2R primer pair has been verified by sequencing to result in a product specific for the PTH2R (Bago et al., 2008). The primer pair for the housekeeping gene glyceraldehyde-3-phosphate dehydrogenase (GAPDH) was 5′-CCACCCAGAAGACTGTGGAT-3′ and 5′-CCCTGTTGCTGTAGCCAAAT-3′ resulting in a PCR product of 423 bp that corresponds to bp 650–1072 of human GAPDH (GeneBank accession number NM_002046). The PCR reactions were performed with iTaq DNA polymerase (Bio-Rad Laboratories, Hercules, CA) in total volumes of 12.5 μl using primers at 300 nM final concentration under the following conditions: 95 °C for 3 min, followed by cycles of 95 °C for 0.5 min, 60 °C for 0.5 min and 72 °C for 1 min. The presence the PTH2R was evaluated after 38 cycles while the presence of GAPDH after 33 cycles. Equal amounts (10 μl) of PCR products were run on gels and pictures taken with a digital camera. Primers for PTH2R are specific to sequences in different exons to allow recognition of potential genomic DNA contamination by the larger size of the product.

Immunolabeling of PTH2R in human tissue

For immunocytochemistry, coronally oriented tissue blocks of about 10×10×20 mm from 3 human brains were sectioned in the coronal plane (Table 1). One tissue block containing insular cortex and continuous tissue blocks from the rostral end of the diencephalon (from 1 mm rostral to the anterior commissure) to the caudal end of the brainstem from a 10 year old male was sectioned. Another tissue block comprising the entire hypothalamus from the brain of an 8 year old female was sectioned. In addition, 2 tissue blocks from a 62 year old male containing the caudal part of the medulla oblongata (from the level of the obex) to the rostral part of the cervical spinal cord were also sectioned.

Two days before sectioning, the tissue blocks were transferred to PB for 2 days to remove the excess paraformaldehyde. Subsequently, the blocks were placed in PB containing 20% sucrose for 2 days for cryoprotection. Then, the blocks were frozen, and cut into 50 μm thick serial coronal sections on a sliding microtome. Immunolabeling was performed as described previously (Dobolyi et al., 2006a) on every 10th section. Briefly, the free-floating sections were pretreated with 3% bovine serum albumin in PB containing 0.5% Triton X-100 for 30 min at room temperature. The sections were then placed in anti-PTH2R primary antiserum (1:20000 dilution) for 48 h at room temperature. This antiserum has previously been used and characterized. It produced strong specific immunolabeling of HEK293 cells stably expressing the human PTH2R and its labeling was blocked by absorption with the peptide immunogen (Usdin et al., 1999a, Wang et al., 2000). Following the incubation in anti-PTH2R primary antiserum, the sections were placed in biotinylated anti-rabbit secondary antibody (1:600 dilution; Vector Laboratories, Burlingame, CA) for 2 h followed by incubation in a solution containing avidin–biotin–peroxidase complex (1:300 dilution; Vector Laboratories) for 2 h. The sections were then treated with fluorescein isothiocyanate (FITC)-tyramide (1:8000 dilution) and H_2O_2 (0.003%) in Tris hydrochloride buffer (0.05 M, pH 8.2) for 6 min. The sections were then mounted, dried, and coverslipped in antifade mounting medium (Prolong Antifade Kit, Molecular Probes, Eugene, OR).

Double immunolabeling of PTH2R and corticotropin-releasing hormone or somatostatin in human hypothalamus

A second set of hypothalamic sections from the 10-year old human was used for double immunolabeling. First, PTH2R immunolabeling was performed as for single labeling except for using more dilute anti-PTH2R primary antiserum (1:40000 dilution), as suggested previously (Hunyady et al., 1996). Subsequently, the sections were incubated in rabbit anti-CRH antibody (Peninsula Laboratories Inc., San Carlos, California; catalogue number T-4037, lot number 041048-5; 1:6000) or rabbit anti-somatostatin antibody (Peninsula Laboratories Inc.; catalogue number T-4103, lot number 010965-7; 1:2000). The antigen sequence of the anti-CRH antibody is H-Ser-Glu-Glu-Pro-Pro-Ile-Ser-Leu-Asp-Leu-Thr-Phe-His-Leu-Leu-Arg-Gl-Val-Leu-Glu-Met-Ala-Arg-Ala-Glu-Gln-Leu-Ala-Gln-Gln-Ala-His-Ser-Asn-Arg-Lys-Leu-Met-Glu-Ile-Ile-NH_2. This antibody recognizes human and rat CRH with equal specificity. Its cross reactivity is 10% to porcine CRH, 5% to savagine, 0.05% to ovine and bovine CRH, and it does not recognize human prepro-CRH, adrenocorticotropin, and PACAP. The antigen sequence of the anti-somatostatin antibody is H-Ala-Gly-Cys-Lys-Asn-Phe-Phe-Trp-Lys-Thr-Phe-Thr-Ser-Cys-OH (disulfide bond). This antibody recognizes somatostatin-14, 28, 25 and (Des-Ala^1)-somatostatin-14 with equal specificity. Its cross reactivity is 0.05% to (D-Trp^8)-somatostatin-14, 0.002% to porcine pro-somatostatin (1–32), and it does not recognize substance P, neuropeptide Y, human, bovine, porcine and rat vasoactive intestinal peptides, human insulin, human amylin, and human, bovine, and porcine glucagon (1–29). The specificity of the anti-CRH and anti-somatostatin antibodies was also supported by the expected well-known distribution of labeled cell bodies in the hypothalamic paraventricular and periventricular nuclei, respectively. Following incubation in primary antibodies, the sections were washed, and CRH or somatostatin was visualized by incubating the sections in Alexa Fluor 594 anti-rabbit secondary antibody (Molecular Probes, 1:500) for 2 hours. Finally, sections were mounted and coverslipped, as described above for single PTH2R labeling.

Macaque tissue

Tissue collection and all procedures were performed according to protocols approved by the Animal Care and Use Committee of the National Institute of Mental Health following ethical review, and in accordance with the Institute for Laboratory Animal Research Guide for the Care and Use of Laboratory Animals. The authors further attest that all efforts were made to minimize the number of animals used and their suffering. A 3-day old male macaque monkey (Macaca mulatta) was sedated with ketamine and then euthanized by i.v. administration of an overdose of pentobarbital. The testis was dissected for the preparation of hybridization probes and the brainstem was dissected for *in situ* hybridization histochemistry. Tissues were frozen and stored at −80 °C until sectioning.

Immunohistochemistry was performed on sections from a 9-year old male macaque that had been used for unrelated physiology experiments. Following deep pentobarbital anesthesia this animal was perfused transcardially with saline followed by 4% paraformaldehyde in 0.1 M PB, at pH 7.4 (PB). Once the brain was removed, it was cryo-protected by first placing it into a 10% glycerol + 2% dimethyl-sulfoxide in PB for 24 hours and then transferring it into a 20% glycerol + 2% dimethyl-sulfoxide in PB for 5 days. The brain was then cut into blocks, frozen, and stored at −80 °C until sectioning.

Different aged monkeys were used for the *in situ* hybridization and immunolabeling experiment because we wanted to minimize the number of animals euthanized. Since, in rats, the expression level of TIP39 is the highest during early postnatal period and no variation with age in PTH2R expression was observed (Dobolyi et al., 2006b), and our experience with in situ hybridization is with fresh frozen material, a brain from a 3 day-old monkey was directly frozen for the

detection of TIP39 and PTH2R mRNA by in situ hybridization. We obtained perfusion fixed material from the brain of a 9 year-old macaque already euthanized for unrelated purposes to avoid euthanizing an animal for PTH2R immunolabeling.

Macaque probe preparation for in situ hybridization

Template cDNA was prepared from macaque testis by an RT reaction, as described above. PCR reactions were also performed essentially as described above using primers with human TIP39 (5′-GGGGACTGTGCGGGAAGC-3′ and 5′-GCATGTACGAGTTCAGCCAGTGG-3′) and PTH2R (5′-TGTGGGGCTTCATCTTGATAGG-3′ and 5′-ATGGCGGTGTCCTTTTCCAGTC-3′) sequences. The PCR products were cloned into plasmid vectors, and their identities were confirmed by DNA sequencing. A plasmid for each probe was used as template in PCR reactions, using primers that appended a T7 RNA polymerase recognition sequence (5′-GCGCGTAATACGACTCACTATAGGG-3′) into the 5′ end of the antisense primer. The TIP39 probe was a 372 base amplicon, which differed from the predicted human sequence (GenBank accession number NM_178449) at 16 scattered base positions. It also lacked codons for two amino acid residues in the predicted leader sequence. The PTH2-R probe was a 500 base amplicon. It differed from the predicted human sequence (GenBank accession number NM_005048) at 14 bases. It also contained a 49 base insertion that corresponds to predicted intronic sequence. The small number of differences between the macaque probes and predicted human sequences may reflect PCR error or artifacts that do not affect their use as probes, or genuine species differences. Sequencing was performed by the NINDS Intramural DNA Sequencing Core Facility.

In situ hybridization histochemistry in macaque

Serial coronal sections (12 μm) were cut from a macaque tissue block using a cryostat. Sections were collected from the rostral border of the diencephalon (about 1 mm rostral to the cross-over level of the anterior commissure) to the caudal border of the pons (about 17 mm caudal to the anterior commissure) mounted on positively charged slides (SuperfrostPlus®, Fisher Scientific, Pittsburgh, PA), dried, and stored at −80°C until use. The distance between sections used for mapping TIP39 and PTH2R mRNA was 240 μm. Antisense (^{35}S)UTP-labeled riboprobes were generated using T7 RNA polymerase from a MAXIscript transcription kit (Ambion, Austin, TX) with TIP39 or PTH2R templates described above. We have shown previously in rat that an antisense probe corresponding to the same region of TIP39 produces equivalent hybridization patterns to probes with non-overlapping sequences corresponding to amino acids −55 to −18, and −17 to 37 (Dobolyi et al., 2003b). Similarly, we have shown in rat that the antisense probe corresponding to the same region of PTH2R produces equivalent hybridization patterns to probes with the non-overlapping sequence corresponding to bases 1274–1828 in rat (Wang et al., 2000). For hybridization, we used 80μl hybridization buffer and 1 million DPM labeled probe per slide. The *in situ* hybridization protocols have been described in detail, elsewhere (http://intramural.nimh.nih.gov/lcmr/snge/Protocols/ISHH/ISHH.html). Following hybridization and washes, slides were dipped in NTB nuclear track emulsion (Eastman Kodak, Rochester NY) and stored at 4°C for 3 weeks. Then, the slides were developed and fixed with Kodak Dektol developer and Kodak fixer, respectively, and counterstained with Giemsa stain, and coverslipped with Cytoseal 60 mounting medium (Stephens Scientific, Riverdale, NJ).

Immunolabeling in macaque tissue

Sections from the 9-year old macaque had been cut in the coronal plane on a sliding microtome at a thickness of 40 μm and stored at −20 °C in a solution of 30% ethylene glycol + 20% glycerol in 0.05 M PB. For double labeling PTH2R and VGLUT2 immunolabeling was performed on

sections extending from the level of the anterior commissure to the end of the hypothalamus, essentially with the same procedure as for single labeling of the PTH2R described above, followed by antigen retrieval and fluorescent immunolabeling of the vesicular glutamate transporter 2 (VGLUT2). Briefly, after FITC-tyramide immunolabeling of the PTH2R, the sections were placed in 10 mM citric acid buffer, pH 6.0 for 30 min at room temperature followed by incubation at 90 °C for 15 min. Subsequently, the sections were placed in anti-VGLUT2 primary antiserum (1:10,000 dilution; a gift from Dr. Robert Edwards, UCSF, CA) for 48 h, at 4 °C. This antiserum was developed against a fusion protein containing glutathione S-transferase and the carboxy-terminal 64 amino acids (residues 519–582) of rat VGLUT2 (Fremeau et al., 2001). It has been used and characterized extensively (Fremeau et al., 2001, Hartig et al., 2003) and Western blot analysis demonstrated that this antibody specifically recognizes VGLUT2 (Fremeau et al., 2001). Following the incubation in the anti-VGLUT2 primary antibody, the sections were incubated in carbocyanine (Cy)-5 conjugated anti-rabbit secondary antibody (1:300 dilution; Vector Laboratories) for 5 hours followed by incubation in 4′,6-diamidino-2-phenylindole (DAPI) for 5 min. The sections were then mounted, dried, and coverslipped in polyvinyl alcohol (PVA) – 1,4-diazabicyclo-2,2,2-octane (DABCO) antifade mounting medium. Control immunostaining, in which the VGLUT2 primary antibody was omitted, was used to verify that the Cy-5 labeling derives from the presence of VGLUT2.

Microscopic analysis

Sections labeled by *in situ* hybridization histochemistry were examined using a Zeiss Axioplan 2 and an Olympus IX70 microscope. Photomicrographs were captured at 1300 × 1030 pixel resolution with an AxioCam HR camera or a Roper CoolSnap FX camera. Montages were created using a Zeiss Axiovision software. Other sections were examined using an Olympus BX60 microscope also equipped with fluorescent epi-illumination. Images were captured at 2048 × 2048 pixel resolution with a SPOT Xplorer digital CCD camera (Diagnostic Instruments, Sterling Heights, MI). Photomicrographs were taken using a 4X objective for fluorescent and dark-field, and 20X or 40X objectives for bright-field images. Confocal images were acquired with a Nikon Eclipse E800 confocal microscope equipped with a BioRad Radiance 2100 Laser Scanninig System using a 60X objective at an optical thickness of 2 μm. Contrast and sharpness of the images were adjusted using the “levels” and “sharpness” commands in Adobe Photoshop CS 8.0. The full resolution was maintained until the micrographs were cropped and assembled, at which point images were adjusted to a resolution of 300 dpi. Drawings were prepared by aligning the pictures with corresponding schematics adapted from a macaque brain atlas (Martin and Bowden, 1996).

RESULTS

Mapping of the expression of the PTH2R in the human brain by RT-PCR

Human brain tissue samples yielded 2–10 μg total RNA. When run on denaturing formaldehyde gels, the intensity of the 28S rRNA band was at least equal to that of the 18S rRNA band in all RNA samples, suggesting acceptable RNA quality. When these RNA samples were reverse transcribed and amplified using PTH2R specific primer pairs, a single band appeared, as shown in figure 1. The PCR product length corresponded to the expected 440 bp suggesting appropriate specific PCR products for the primer pair, which was also confirmed by sequencing. A band with high intensity signal was found for samples from the septum, the caudate nucleus, the medial geniculate body, the medial hypothalamus, the pretectal area, the pontine tegmentum, and the cerebellar cortex (Fig. 1). A lower intensity band was found for the frontal cortex, hippocampus, amygdala, lateral geniculate body, subthalamic nucleus, ventral tegmental area, dorsal vagal complex, and the spinal trigeminal nucleus (Fig. 1). In contrast, no band was detected for the ventral thalamus, the mediodorsal thalamic nucleus, the pulvinar, the substantia nigra, the pontine nuclei, the ventrolateral medulla, and the inferior

olive (Fig. 1). There were 9 brain regions analyzed in samples from 2 different brains. Samples from the hippocampus, the subthalamic nucleus, and the pontine reticular formation resulted in indistinguishable PCR bands. The ventral thalamus, the mediodorsal thalamic nucleus, and the pontine nuclei did not contain detectable PTH2R mRNA in either brain. The pretectal area, the pontine tegmentum, and the cerebellar cortex were also all positive for PTH2R but the intensity of the band was lower in the samples from the second brain. Using primers specific for the housekeeping gene GAPDH resulted in bands of the expected length of 423 bp with about the same intensity for all the samples except for the no RNA negative control (Fig. 1).

Distribution of PTH2R immunoreactivity in the human brain

PTH2R-ir fibers had a widespread distribution in several brain areas, as described below (Table 2).

Cerebral cortex—The insular cortex was examined and only a few scattered PTH2R-ir fibers were detected.

Thalamus—The thalamus had a relative paucity of PTH2R-ir fibers (Table 2). High densities of PTH2R-ir fibers were only detected in the paraventricular thalamic nucleus (Fig. 2H). In addition, a few PTH2R-ir fibers were scattered in the anteromedial, lateral, posterior, and suprageniculate thalamic nuclei, in the habenula, the peripeduncular area, and the lateral geniculate body.

Hypothalamus—In general, the hypothalamus contained dense areas of PTH2R-ir nerve fibers and terminals (Table 2). A particularly dense network of PTH2R-ir fibers was seen in the medial preoptic area (Fig. 2B), in contrast to the low density in the lateral preoptic area. The paraventricular (Fig. 2D) and infundibular nuclei (Fig. 2E) also contained a very dense fiber network, with PTH2R-ir fibers projecting towards the median eminence where very intense PTH2R immunolabeling was visible, particularly in the external layer (Fig. 2F). Immunopositive fibers were also numerous throughout the entire lateral hypothalamic area (Fig. 2I), the supraoptic (Fig. 2B), dorsomedial, posterior hypothalamic, tuberomamillary and premamillary nuclei. A moderate to high density of PTH2R-ir fibers were present in the anterior hypothalamic, ventromedial, perifornical, and subthalamic nuclei, as well as in the nuclei of the mamillary body (Fig. 2I), whereas only a few scattered PTH2R-ir fibers were detected in the suprachiasmatic nucleus (Fig. 2B).

Midbrain—The highest density of PTH2R-ir fibers in the midbrain was within the periaqueductal gray. PTH2R-ir fibers formed networks in the dorsomedial and lateral subdivision, whereas the number of PTH2R-ir fibers was lower in the dorsolateral and ventral subdivisions (Fig. 3D). Other midbrain regions that contained a relatively high density of PTH2R-ir fibers include the zona incerta, the subbrachial nucleus, the pretectal area, the superior and inferior colliculi, and the ventral tegmental area. The dorsal raphe nucleus had a considerably lower density of PTH2R-ir fibers, but no PTH2R immunoreactivity was present in the substantia nigra, the red nucleus, and the oculomotor nuclei.

Pons—PTH2R-ir fibers were densely packed in the lateral parabrachial nucleus (Fig. 3B). A much lower density of PTH2R-ir fibers was seen in the tegmentum and the sensory trigeminal nuclei. In addition, solitary PTH2R-ir fibers were scattered in the pontine reticular formation, the pontine raphe nucleus, the nuclei of the superior olive and the vestibular nuclei.

Medulla oblongata—A very dense network of PTH2R-ir fibers was seen in the marginal layer of the spinal trigeminal nucleus (not shown). In addition, a high density of PTH2R-ir fibers was present in the nucleus of the solitary tract immediately adjacent to the area postrema

and in the dorsal reticular nucleus of the medulla. Some PTH2R-ir fibers were also distributed in the area postrema. In addition, scattered fibers were present in the different compartments of the medullary reticular formation.

Spinal cord—In sections of the spinal cord, laminae I and II in the dorsal horn showed strikingly intense immunolabeled varicose fibers (Fig. 3E). Lamina X and the intermediomedial nucleus contained a few lightly labeled fibers. Scattered fibers were present in all of the deep layers of the dorsal horn and a few fibers were also present in the ventral horn.

Relationship between the PTH2R and somatostatin-, and CRH-containing hypothalamic neurons in human

Somatostatin-ir perikarya were distributed in the hypothalamic periventricular nucleus surrounded by somatostain-ir fibers projecting ventrally towards the medial basal hypothalamus and the median eminence (Fig. 4A). Double immunolabeling revealed that a portion of these somatostatin-ir fibers contain PTH2R-ir while other fibers contained either only somatostatin, or only PTH2R-ir (Fig. 4A,B).

A very high density of both somatostatin-ir and PTH2R-ir fibers was present in the median eminence (Fig. 4C). The vast majority of PTH2R-ir fiber terminals in the median eminence contained somatostatin, as demonstrated by high magnification images of double-immunostained sections (Fig. 4C). In contrast, only a portion of somatostatin-ir fiber terminals in the median eminence showed co-localization with PTH2R-ir (Fig. 4C).

CRH-ir cell bodies and fibers were distributed in the hypothalamic paraventricular nucleus (Fig. 4D,E). Double immunolabeling demonstrated that CRH-ir cell bodies and fibers do not contain PTH2R immunoreactivity (Fig. 4E). However, PTH2R-ir fiber terminals closely apposed CRH-ir perikarya (Fig. 4E).

Distribution of PTH2R mRNA in the macaque brain by *in situ* hybridization histochemistry

Basal ganglia and other forebrain structures—Some of the most rostral sections allowed us to analyze PTH2R-expressing neurons in the hippocampus, the amygdala, and some of the basal ganglia. Only a few scattered PTH2R-expressing neurons were visible in the hippocampus, distributed throughout the dentate gyrus and the hippocampal areas. In contrast, the amygdala contained a very high density of PTH2R-expressing neurons in the central amygdaloid nucleus (Fig. 5C), while PTH2R-expressing neurons were also abundant in the medial amygdaloid nucleus (Fig. 5C). Other regions of the amygdala contained significantly lower levels of PTH2R mRNA. Also, a low density of PTH2R-expressing neurons was found in the caudate nucleus and the substantia innominata while the putamen and the internal and external parts of the globus pallidus did not contain PTH2R mRNA (Fig. 5C).

Thalamus—In general, the thalamus showed very modest PTH2R mRNA labeling with the exception of its metathalamic portion, the medial geniculate body. Here, PTH2R-expressing neurons had a very high density in the medial nucleus of the medial geniculate body, a somewhat lower density in the ventral nucleus (Fig. 5E), and adjacent suprageniculate thalamic nucleus and no labeling in the dorsal nucleus. In addition, PTH2R-expressing cells were present, at low density, in the midline thalamic nuclei, particularly in the paraventricular thalamic nucleus, the lateral habenular nucleus, the peripeduncular area, and the lateral geniculate body. The anterior, lateral, ventral, and posterior thalamic cell groups did not show PTH2R mRNA labeling (Table 2).

Hypothalamus—*In situ* hybridization indicated that the hypothalamus was rich in PTH2R-expressing neurons. A very high density of PTH2R-expressing neurons was found in the medial preoptic nucleus while other regions of the preoptic area exhibited a low density of labeled neurons (not shown). A very high intensity of PTH2R mRNA labeling was also seen in the hypothalamic paraventricular nucleus, particularly in its parvicellular subdivisions (Fig. 5B). Labeled neurons extended into the hypothalamic periventricular nucleus, albeit in a significantly smaller number (Fig. 5B). A cluster of intensely labeled PTH2R-expressing neurons was also detected in the ventral part of the lateral hypothalamic area (Fig. 5B). Many other parts of the hypothalamus showed only a low density of PTH2R-expressing neurons including the supraoptic, anterior hypothalamic, infundibular, ventromedial, dorsomedial, perifornical, posterior hypothalamic, tuberomamillary, and premamillary nuclei. PTH2R-expressing cells were scarce in the mamillary body and the subthalamic nucleus. Some neurons of the superior but none in the medial or lateral mamillary nuclei contained PTH2R mRNA.

Midbrain—PTH2R-expressing cells were abundant in several different midbrain regions. The superior colliculus contained a very high density of PTH2R-expresing cells in its superficial layers and fewer labeled neurons in the deep layers (Fig. 6B). Similarly, the PTH2R-expressing neurons were topographically organized in the periaqueductal gray as well. The lateral subdivision demonstrated a high density of labeled neurons while other subdivisions contained fewer PTH2R-expressing neurons (Fig. 6C). The dorsal raphe nucleus also had a strong PTH2 receptor mRNA *in situ* hybridization signal (Fig. 6D). In addition, densely packed PTH2R-expressing neurons were apparent in the entire length of the parabigeminal nucleus (Fig. 6E). Several other regions of the midbrain contained a low to moderate density of PTH2R-expressing cells, including the zona incerta, the ventral tegmental area, the subbrachial nucleus, and the inferior colliculus. No labeled neurons were found in the substantia nigra, the red nucleus, or the oculomotor nuclei (Table 2).

Pons—The pons had few PTH2R-expressing neurons except for the dorsal tegmental nucleus, which contained a relatively high level of PTH2R mRNA. Labeled neurons were sparsely distributed in other parts of the pontine tegmentum, the parabrachial nuclei, the pontine reticular formation, and the sensory trigeminal nucleus.

Vesicular glutamate transporter 2 immunoreactivity in PTH2R-containing fiber terminals in macaque

In the regions of the macaque brain examined, which extended from the level of the anterior commissure to the caudal end of the diencephalon, PTH2R-ir fibers were abundant in the ventral part of the lateral septal nucleus and in the same regions of the thalamus and hypothalamus, as described in human. In addition, some scattered fibers were present in cortical areas. In some regions, including the lateral septum and preoptic area (Fig 7) double-labeling revealed that essentially all PTH2R-ir fiber terminals contained VGLUT-ir.

Distribution of TIP39 mRNA in the macaque brain by *in situ* hybridization histochemistry

Numerous TIP39 mRNA containing neurons were found in the posterior thalamus. One group of these neurons was located in the subparafascicular area between the most caudal portion of the third ventricle and the fasciculus retroflexus (Fig. 8B). Additional TIP39-expressing neurons were found lateral to the fasciculus retroflexus (Fig. 8B) in the parvicellular subparafascicular nucleus distributing along the dorsal edge of the medial lemniscus. These neurons extended laterally as far as the peripeduncular area immediately ventromedial to the medial geniculate body.

Another group of TIP39-expresing neurons was located medial to the dorsal part of the ventral nucleus of the lateral lemniscus at the midbrain-pons junction (Fig. 8D). The topography of

these TIP39-expressing neurons corresponds to the medial paralemniscal nucleus, as it has been identified in rodents (Dobolyi et al., 2003b,Varga et al., 2008).

DISCUSSION

The major purpose of this study was to provide a comparison of the neuroanatomical distribution of the PTH2R and TIP39 in human and non-human primates with their distributions in rodents. We are experimentally evaluating this neuromodulator system in rodents and performed this comparison to help evaluate the potential extrapolation of its functions in rodents to humans. We focused on material and brain regions most likely to be informative in this regard. The major finding is that both the PTH2R and TIP39 have a similar distribution in human and macaque to their distributions in rodents. Their expression is greatest in subcortical structures. The data supports the idea that they may be involved in similar functions. However, judgment about the relevance of particular observations made in rodents to humans obviously requires detailed consideration of the relevant functions and structures.

In the following discussion the distribution of PTH2R mRNA obtained with different methods and in different material is compared. Next, the distribution of PTH2R immunoreactivity is compared between the human and non-human primate material used in this study and published rodent data. Finally, the expression of TIP39 and the presence of TIP39-PTH2R neuromodulator system in primates are discussed with a view of potential functional implications.

Distribution of the expression of PTH2R mRNA in the primate brain

PTH2R mRNA was detected with 2 different methods, RT-PCR in the brain of adults and *in situ* hybridization histochemistry in 3-day old macaque monkey. The rationale for comparing these distributions is that the expression level of the PTH2R did not change during postnatal development in the rat (Dobolyi et al., 2006b). However, we consider some methodological issues of detecting mRNA of the PTH2R before comparing RT-PCR and *in situ* hybridization data.

Methodological considerations—The RT-PCR experiments were designed so that the appearance of a PTH2R band in the gel means that PTH2R mRNA was present in the microdissected tissue sample while the absence of a band is a good indication of the absence PTH2R mRNA. First, the mRNA quality was checked for each human sample to eliminate the possibility that mRNA degradation in the post-mortem period would lead to a negative signal. In addition, the presence of the house-keeping gene GAPDH was shown in each sample using a lower cycle number to demonstrate that mRNA was efficiently transcribed into cDNA. In contrast, a high cycle number was used for the PTH2R so that even a small amount of mRNA would be detected. For the better comparison of the PTH2R expression in different samples, the RNA concentrations were measured and adjusted so 2 μg was used for each sample. A negative control sample without RNA was used to exclude the possibility of contamination at either the RNA or the cDNA level. Furthermore, an intron spanning PTH2R primer pair was used to create larger PCR product amplified from genomic DNA so potential genomic contamination would be recognized. Finally, the specificities of the PCR products were demonstrated by sequencing. The reproducibility of our data were also confirmed when 9 samples of the same brain regions were analyzed from 2 different human brains. Indistinguishable results were obtained for 6 samples while 3 samples produced clear bands from both brains that differed in their intensity. Since PTH2R expression does not obviously vary with gender or age in rat (Dobolyi et al., 2006b), it is possible that methodological reasons account for these small differences. For example, microdissection from different parts of the same nucleus could result in different intensity PTH2R bands if the expression level of PTH2R

varies topographically within a single brain nucleus or region. Such topographical differences were indeed revealed by *in situ* hybridization in the macaque brain in various brain regions including the amygdala, the hypothalamus, the medial geniculate body, the periaqueductal gray, the superior colliculus, and the pontine tegmentum.

Comparison of RT-PCR and in situ hybridization data—PTH2R mRNA has a widespread expression in the brain of both human and non-human primates based on the results of both the RT-PCR and *in situ* hybridization experiments (Table 1). Cortical structures seem to contain some PTH2R mRNA while the PTH2R expression level was high in the septum and the caudate nucleus based on RT-PCR data in human. In the amygdala, RT-PCR showed a moderate level of PTH2R expression while *in situ* hybridization demonstrated high levels of PTH2R expression in the central and medial nuclei, with only low levels in other nuclei of the amygdala. Thalamic nuclei including the ventral nuclei, the mediodorsal thalamic nucleus, and the pulvinar do not express PTH2R based on the RT-PCR and *in situ* hybridization histochemical data. These two techniques also provided consistent data on a high level of PTH2R mRNA in the medial geniculate body, the medial hypothalamus, and the pontine tegmentum and a low level of PTH2R expression in the lateral geniculate body, the subthalamic nucleus, the ventral tegmental area, and the pontine reticular formation. Furthermore, neither technique reported mRNA in the substantia nigra or in the pontine nuclei. In general, a very good agreement between the results of the two techniques confirms the findings. The only apparently contradictory findings were that the pretectal area, where RT-PCR suggested a high level of PTH2R mRNA expression, failed to show any labeling by using *in situ* hybridization histochemistry. This difference could be the result of using adult human brain tissue for RT-PCR and macaque brain for *in situ* hybridization histochemistry as overall similarities with small differences have also been reported between the mRNA distribution of other neuropeptide systems in macaque and human (Hurd et al., 1999). The generally good agreement between the RT-PCR and *in situ* hybridization data, however, argues that the distribution of PTH2R expression is very similar in macaque and human, and is consistent with previous observations in rat that PTH2R expression levels do not change during postnatal development (Dobolyi et al., 2006b).

Comparison of the distribution of the PTH2R mRNA in primates and rodents—The pattern of the PTH2R expression in the brain of primates is generally similar to that previously reported in mice (Faber et al., 2007). The high expression levels of the PTH2R in the septum, the caudate nucleus, the medial geniculate body, the hypothalamus, the pontine tegmentum, and the cerebellum, the lower expression levels in the cerebral cortex, the hippocampus, the amygdala, the lateral geniculate body, the ventral tegmental area, the pontine reticular formation, the dorsal vagal complex, and the spinal trigeminal nucleus, as well as the absence of PTH2R mRNA in most thalamic nuclei, the suprachiasmatic nucleus, the medial and lateral mamillary nuclei, the substantia nigra, the red nucleus, the brainstem motor nuclei, and most pontine and medullary regions are all consistent with the level of PTH2R expression in the corresponding brain regions in mice (Faber et al., 2007). *In situ* hybridization histochemistry revealed that the subregional distribution of PTH2R mRNA in macaque is often similar to that in mice. In the medial geniculate body, the medial nucleus had the highest density of PTH2R expressing cells with some limited expression in the ventral nucleus and no expression in the dorsal nucleus in both macaque and mice. In the hypothalamus, similarly high expression levels were also found in the medial preoptic area and the paraventricular and periventricular nuclei in both species. Such similarities between mRNA distributional patterns in rodents and primates are not uncommon and have also been reported for other neuropeptides and neuropeptide receptors (Elias et al., 2001, Cunningham et al., 2002). Nevertheless, there were two regions, namely the ventral part of the lateral hypothalamus and the parabigeminal

nucleus where PTH2R-expressing cells formed compact cell groups in the macaque while only scattered labeled cells were found in rodents, suggesting some species differences.

PTH2R immunoreactivity in the primate brain

PTH2R in fiber terminals vs. cell bodies—In rat immunolabeling of the PTH2R with FITC-tyramide amplification recognizes all structures described with traditional DAB visualization of immunoreactivity and also reveals additional fine fibers not detected otherwise (Dobolyi et al., 2006a). Cell bodies were not detectable by immunolabeling of the PTH2R in human. This was also the case in mouse, and in this species the positions of the PTH2R-expressing cells were established by *in situ* hybridization as well as by the distribution of beta-galactosidase driven by the PTH2R promoter in knock-in mice (Faber et al., 2007). The lack of immunolabeling within the neuronal perikarya may indicate that PTH2R protein is promptly transported after its synthesis towards the fiber terminals, as it has also been suggested in the case of several other receptors (Deuchars et al., 2001, Stanic et al., 2006). In contrast to most brain regions where PTH2R-immunoreactive fibers were found together with PTH2R mRNA expressing cells, the caudate nucleus contained a significant amount PTH2R mRNA in primates, as well as in mice (Faber et al., 2007) but no PTH2R-ir fibers (Table 2.) suggesting that the PTH2R is expressed in neurons of the caudate nucleus that projects to other brain regions and that the techniques for detection of mRNA are more sensitive than those for protein.

Distribution of PTH2R-ir fibers and fiber terminals—We described PTH2R-ir fibers in the several different brain regions of human and macaque including endocrine hypothalamic structures, such as the median eminence, the infundibular, the hypothalamic paraventricular, and periventricular nuclei. Another brain region with a high density of PTH2R-ir fibers, the medial preoptic area, also contains hypophysiotropic neurons and participates in additional hypothalamic functions, including the regulation of reproductive behaviors (Swann et al., 2003, Pfaff et al., 2006). PTH2R-ir fibers and fiber terminals were also abundant in other brain regions involved in multiple brain functions including the lateral septal nucleus, the paraventricular thalamic nucleus, and the periaqueductal gray. Finally, PTH2R-ir fibers appeared in somato- and viscerosensory centers, including the superficial laminae of the spinal cord dorsal horn, the sensory trigeminal nuclei, the nucleus of the solitary tract, and the lateral parabrachial nucleus. These topographical arrangements of PTH2R-ir fibers and terminals in primates, like the distribution of receptor synthesizing cells, are very similar to that in rodents. Such similarities between distributional patterns in the brains of primates and rodents have often been reported for other neuropeptides and neuropeptide receptors suggesting similar functions in different species (de Lacalle and Saper, 2000, Kostich et al., 2004).

Glutamatergic nature of PTH2R-ir fiber terminals—The quantal release of glutamate depends on its transport into synaptic vesicles. Therefore, the presence of vesicular glutamate transporters in nerve terminals can be used as markers of glutamatergic presynaptic terminals (Fremeau et al., 2001). In septal and hypothalamic regions, most glutamatergic terminals contain VGLUT2 in the rat (Lin et al., 2003). In the macaque, we observed a very dense network of VGLUT2 -ir fiber terminals in septal and hypothalamic regions. Some of these terminals also contained PTH2R-ir and essentially all PTH2R-ir-containing terminals in those areas contained VGLUT2-ir. The co-localization of PTH2R-ir and VGLUT2-ir suggests that PTH2R-ir-containing terminals in the septum, hypothalamus, and perhaps other areas are glutamatergic presynaptic terminals.

The TIP39-PTH2R neuromodulator system in primates

TIP39-expressing neurons were present in the subparafascicular area and in the medial paralemniscal nucleus in 3-day old macaque similar to the positions of TIP39-expressing cells in rodents. We did not detect TIP39 mRNA in human brain but the most likely explanation is

that the level of TIP39 decreases during postnatal development in primates similar to that previously reported in rodents (Dobolyi et al., 2006b, Brenner et al., 2008). We were not able to obtain young human samples for RNA detection from the two brain regions containing TIP39 neurons in rodent and monkey. Knowing that PTH2R synthesizing cells bodies, PTH2R containing fibers, and TIP39 synthesizing cell bodies have essentially the same distribution in non-human primates and rodent, that TIP39 fibers project to PTH2R rich regions in rodents, and that PTH2R fibers have a similar distribution in rodents, human and non-human primates it seems likely that there is a similar TIP39/PTH2R match in human and non-human primates as well. Thus, subparafascicular TIP39 neurons likely project to limbic and endocrine brain regions, while medial paralemniscal TIP39 neurons project to auditory and viscerosensory centers, as it has been demonstrated in rodents (Dobolyi et al., 2003a). Furthermore, the data also suggest that even though the human PTH2R, in contrast to the rat PTH2R, can bind human PTH as well as human TIP39 (Usdin et al., 1999b), TIP39 is the physiological ligand of the PTH2R in primates, at least in the brain.

The TIP39-PTH2R neuromodulator system may exert its action on neuronal function by presynaptic modulation. The transport of the PTH2R protein into axon terminals supports a role of the receptor in presynaptic modulation, as previously suggested in rodents based on the presynaptic location of the PTH2R, as well as on the matching subregional distribution of TIP39-ir and PTH2R-ir axon terminals (Dobolyi et al., 2006a, Faber et al., 2007). The presynaptic modulation by TIP39 may affect the functions of neurons that contain the PTH2R and also neurons that are innervated by PTH2R-containing nerve terminals. Our data provide the anatomical basis for both types of actions of TIP39 on hypothalamic hypophysiotropic neurons. Somatostatin neurons in the hypothalamic periventricular nucleus project to the median eminence where somatostatin is released from their terminals, reaches the anterior pituitary *via* the portal system, and inhibits growth hormone secretion (Bluet-Pajot et al., 1998). The PTH2R content of these terminals provides the possibility that TIP39 directly regulates somatostatin release by acting on these PTH2Rs. Since the activation of the PTH2R leads to increased cAMP and calcium levels (Behar et al., 1996) TIP39 could increase somatostatin release. Such action would be consistent with the inhibitory action of TIP39 on the growth hormone release from the pituitary (Usdin et al., 2003). TIP39 may affect CRH neurons in the paraventricular hypothalamic nucleus by a different mechanism of action. CRH neurons do not contain PTH2Rs, but they are innervated and influenced by glutamatergic synapses (Cole and Sawchenko, 2002, Wittmann et al., 2005). Since the presynaptic terminals of some of these excitatory synapses contain PTH2Rs, TIP39 might increase the excitatory influence on CRH neurons via these PTH2Rs. Such a mechanism is consistent with TIP39 stimulation of CRH secretion from hypothalamic explants (Ward et al., 2001).

Our anatomical data, together with the similarity of the topographical distribution of the TIP39-PTH2R neuromodulator system in primates and rodents, suggest that in primates the TIP39-PTH2R neuromodulator system may be involved in functional activities that have been suggested by studies in rodents including the regulation of fear, anxiety, reproductive behaviors, release of pituitary hormones, and nociceptive information processing (Ward et al., 2001, Dobolyi et al., 2002, Sugimura et al., 2003, Usdin et al., 2003, LaBuda et al., 2004, LaBuda and Usdin, 2004, Palkovits et al., 2004, Wang et al., 2006a, Fegley et al., 2008). In addition, our study implies that future data obtained in rodents can also be realistically extrapolated to human. At present, the only human study related to a brain region in which TIP39 neurons are concentrated is the reported increased regional blood flow during male ejaculation in the human subparafascicular area (Holstege et al., 2003). Based on the anatomical observations in this study, additional investigation of the functional role of the TIP39-PTH2R neuromodulator system in the human brain are expected and required.

In conclusion, our study demonstrates of the presence of PTH2R and TIP39 mRNA in the brain of human and non-human primate, as well as PTH2R immunoreactivity in the human central nervous system. The neuroanatomical distribution of the PTH2R and TIP39 are quite similar in human and non-human primates and rodents.

Acknowledgments

We thank Dr. Robert Edwards for providing the antiserum against VGLUT2. The technical assistance of Dorottya Kézdi and Éva Rebeka Szabó is appreciated. The work was supported by the Hungarian Science Foundation NKTH-OTKA K67646 grant for AD, the consortial FP6 EU Grant BrainNet II LSHM-CT-2004-503039 for MP, and the Intramural Research Program of the NIH, National Institute of Mental Health for TBU. Arpád Dobolyi is grantee of the Bolyai János Scholarship.

Abbreviations in the text

CRH
: corticotropin-releasing hormone

DAPI
: 4′,6-diamidino-2-phenylindole

FITC
: fluorescein isothiocyanate

GAPDH
: glyceraldehyde-3-phosphate dehydrogenase

MPL
: medial paralemniscal nucleus

PB
: phosphate buffer

PTH
: parathyroid hormone

PTHrP
: PTH-related peptide

PTH2R
: parathyroid hormone 2 receptor

SPF
: subparafascicular area

TIP39
: tuberoinfundibular peptide of 39 residues

VGluT2
: vesicular glutamate transporter 2

COMPREHENSIVE LIST OF ABBREVIATIONS

ac
: anterior commissure

AcN
: accumbens nucleus

al
ansa lenticularis

AM
anteromedial thalamic nucleus

APr
anteroprincipal thalamic nucleus

Aq
cerebral aqueduct

BNST
bed nucleus of the stria terminalis

CeA
central amygdaloid nucleus

cp
cerebral peduncle

cu
cuneate fasciculus

DG
dentate gyrus

DH
dorsal horn

dlf
dorsolateral fasciculus

DLPAG
PAG, dorsolateral subdivision

DMH
hypothalamic dorsomedial nucleus

DMPAG
PAG, dorsomedial subdivision

DpMe
deep mesencephalic nucleus

DR
dorsal raphe nucleus

DTg
dorsal tegmental nucleus

EGP
external globus pallidus

f
fornix

fr
fasciculus retroflexus

ic
internal capsule

IGP
internal globus pallidus

Inf
infundibular nucleus

LG
lateral geniculate body

LHA
lateral hypothalamic area

ll
lateral lemniscus

LPAG
PAG, lateral subdivision

LV
lateral ventricle

L2
lamina 2 of the spinal dorsal horn

me
median eminence

MeA
medial amygdaloid nucleus

mfb
medial forebrain bundle

MG
medial geniculate body

mlf
medial longitudinal fasciculus

MMG
medial nucleus of the medial geniculate body

MMN
medial mamillary nucleus

MPA
medial preoptic area

MPN
medial preoptic nucleus

ot
optic tract

Pa
hypothalamic paraventricular nucleus

PAG periaqueductal gray

PBG parabigeminal nucleus

PBL lateral parabrachial nucleus

Pe hypothalamic periventricular nucleus

Pir piriform cortex

Pn pontine nuclei

PnO pontine reticular nucleus, oral part

PP peripeduncular nucleus

Pu putamen

Pul pulvinar thalami

PVT paraventricular thalamic nucleus

py pyramidal tract

Rt reticular thalamic nucleus

Sag sagulum nucleus

SC superior colliculus

SCh suprachiasmatic nucleus

scp superior cerebellar peduncle

SI substantia innominata

sm stria medullaris

SN substantia nigra

SO supraoptic nucleus

SOC superior olivary complex

SPF subparafascicular nucleus

SPFp subparafascicular nucleus, parvicellular part

VA ventroanterior thalamic nucleus

VLL ventral nucleus of the lateral lemniscus

VMG ventral nucleus of the medial geniculate body

VMH hypothalamic ventromedial nucleus

VPL ventral posterolateral thalamic nucleus

3nu motor oculomotor nucleus

3V third ventricle

4n trochlear nerve

LITERATURE CITED

Bago AG, Palkovits M, Usdin TB, Seress L, Dobolyi A. Evidence for the expression of parathyroid hormone 2 receptor in the human brainstem. Ideggyogy Sz 2008;61:123–126. [PubMed: 18459453]

Behar V, Pines M, Nakamoto C, Greenberg Z, Bisello A, Stueckle SM, Bessalle R, Usdin TB, Chorev M, Rosenblatt M, Suva LJ. The human PTH2 receptor: binding and signal transduction properties of the stably expressed recombinant receptor. Endocrinology 1996;137:2748–2757. [PubMed: 8770894]

Bluet-Pajot MT, Epelbaum J, Gourdji D, Hammond C, Kordon C. Hypothalamic and hypophyseal regulation of growth hormone secretion. Cellular and molecular neurobiology 1998;18:101–123. [PubMed: 9524732]

Brenner D, Bago AG, Gallatz K, Palkovits M, Usdin TB, Dobolyi A. Tuberoinfundibular peptide of 39 residues in the embryonic and early postnatal rat brain. J Chem Neuroanat 2008;36:59–68. [PubMed: 18495420]

Cole RL, Sawchenko PE. Neurotransmitter regulation of cellular activation and neuropeptide gene expression in the paraventricular nucleus of the hypothalamus. J Neurosci 2002;22:959–969. [PubMed: 11826124]

Coolen LM, Allard J, Truitt WA, McKenna KE. Central regulation of ejaculation. Physiol Behav 2004;83:203–215. [PubMed: 15488540]

Cunningham MJ, Scarlett JM, Steiner RA. Cloning and distribution of galanin-like peptide mRNA in the hypothalamus and pituitary of the macaque. Endocrinology 2002;143:755–763. [PubMed: 11861493]

de Lacalle S, Saper CB. Calcitonin gene-related peptide-like immunoreactivity marks putative visceral sensory pathways in human brain. Neuroscience 2000;100:115–130. [PubMed: 10996463]

Deuchars SA, Atkinson L, Brooke RE, Musa H, Milligan CJ, Batten TF, Buckley NJ, Parson SH, Deuchars J. Neuronal P2X7 receptors are targeted to presynaptic terminals in the central and peripheral nervous systems. J Neurosci 2001;21:7143–7152. [PubMed: 11549725]

Dobolyi A, Irwin S, Wang J, Usdin TB. The distribution and neurochemistry of the parathyroid hormone 2 receptor in the rat hypothalamus. Neurochem Res 2006a;31:227–236. [PubMed: 16570212]

Dobolyi A, Palkovits M, Bodnar I, Usdin TB. Neurons containing tuberoinfundibular peptide of 39 residues project to limbic, endocrine, auditory and spinal areas in rat. Neuroscience 2003a;122:1093–1105. [PubMed: 14643775]

Dobolyi A, Palkovits M, Usdin TB. Expression and distribution of tuberoinfundibular peptide of 39 residues in the rat central nervous system. J Comp Neurol 2003b;455:547–566. [PubMed: 12508326]

Dobolyi A, Ueda H, Uchida H, Palkovits M, Usdin TB. Anatomical and physiological evidence for involvement of tuberoinfundibular peptide of 39 residues in nociception. Proc Natl Acad Sci U S A 2002;99:1651–1656. [PubMed: 11818570]

Dobolyi A, Wang J, Irwin S, Usdin TB. Postnatal development and gender-dependent expression of TIP39 in the rat brain. J Comp Neurol 2006b;498:375–389. [PubMed: 16871538]

Elias CF, Lee CE, Kelly JF, Ahima RS, Kuhar M, Saper CB, Elmquist JK. Characterization of CART neurons in the rat and human hypothalamus. J Comp Neurol 2001;432:1–19. [PubMed: 11241374]

Faber CA, Dobolyi A, Sleeman M, Usdin TB. Distribution of tuberoinfundibular peptide of 39 residues and its receptor, parathyroid hormone 2 receptor, in the mouse brain. J Comp Neurol 2007;502:563–583. [PubMed: 17394159]

Fegley DB, Holmes A, Riordan T, Faber CA, Weiss JR, Ma S, Batkai S, Pacher P, Dobolyi A, Murphy A, Sleeman MW, Usdin TB. Increased fear- and stress-related anxiety-like behavior in mice lacking tuberoinfundibular peptide of 39 residues. Genes Brain Behav 2008;7:933–942. [PubMed: 18700839]

Fremeau RT Jr, Troyer MD, Pahner I, Nygaard GO, Tran CH, Reimer RJ, Bellocchio EE, Fortin D, Storm-Mathisen J, Edwards RH. The expression of vesicular glutamate transporters defines two classes of excitatory synapse. Neuron 2001;31:247–260. [PubMed: 11502256]

Harmar AJ. Family-B G-protein-coupled receptors. Genome Biol 2001;2:30131–30110.

Hartig W, Riedel A, Grosche J, Edwards RH, Fremeau RT Jr, Harkany T, Brauer K, Arendt T. Complementary distribution of vesicular glutamate transporters 1 and 2 in the nucleus accumbens of rat: Relationship to calretinin-containing extrinsic innervation and calbindin-immunoreactive neurons. J Comp Neurol 2003;465:1–10. [PubMed: 12926012]

Hoare SR, Clark JA, Usdin TB. Molecular determinants of tuberoinfundibular peptide of 39 residues (TIP39) selectivity for the parathyroid hormone-2 (PTH2) receptor. N-terminal truncation of TIP39 reverses PTH2 receptor/PTH1 receptor binding selectivity. J Biol Chem 2000;275:27274–27283. [PubMed: 10854439]

Hoare SR, Usdin TB. Molecular mechanisms of ligand recognition by parathyroid hormone 1 (PTH1) and PTH2 receptors. Curr Pharm Des 2001;7:689–713. [PubMed: 11375776]

Holstege G, Georgiadis JR, Paans AM, Meiners LC, van der Graaf FH, Reinders AA. Brain activation during human male ejaculation. J Neurosci 2003;23:9185–9193. [PubMed: 14534252]

Hunyady B, Krempels K, Harta G, Mezey E. Immunohistochemical signal amplification by catalyzed reporter deposition and its application in double immunostaining. J Histochem Cytochem 1996;44:1353–1362. [PubMed: 8985127]

Hurd YL, Keller E, Sotonyi P, Sedvall G. Preprotachykinin-A mRNA expression in the human and monkey brain: An in situ hybridization study. J Comp Neurol 1999;411:56–72. [PubMed: 10404107]

John MR, Arai M, Rubin DA, Jonsson KB, Juppner H. Identification and characterization of the murine and human gene encoding the tuberoinfundibular peptide of 39 residues. Endocrinology 2002;143:1047–1057. [PubMed: 11861531]

Kostich WA, Grzanna R, Lu NZ, Largent BL. Immunohistochemical visualization of corticotropin-releasing factor type 1 (CRF1) receptors in monkey brain. J Comp Neurol 2004;478:111–125. [PubMed: 15349973]

Kronenberg HM, Lanske B, Kovacs CS, Chung UI, Lee K, Segre GV, Schipani E, Juppner H. Functional analysis of the PTH/PTHrP network of ligands and receptors. Recent Prog Horm Res 1998;53:283–301. [PubMed: 9769712]

LaBuda CJ, Dobolyi A, Usdin TB. Tuberoinfundibular peptide of 39 residues produces anxiolytic and antidepressant actions. Neuroreport 2004;15:881–885. [PubMed: 15073536]

LaBuda CJ, Usdin TB. Tuberoinfundibular peptide of 39 residues decreases pain-related affective behavior. Neuroreport 2004;15:1779–1782. [PubMed: 15257146]

Li C, Chen P, Smith MS. Neural populations in the rat forebrain and brainstem activated by the suckling stimulus as demonstrated by cFos expression. Neuroscience 1999;94:117–129. [PubMed: 10613502]

Lin SH, Miyata S, Matsunaga W, Kawarabayashi T, Nakashima T, Kiyohara T. Metabolic mapping of the brain in pregnant, parturient and lactating rats using fos immunohistochemistry. Brain Res 1998;787:226–236. [PubMed: 9518626]

Lin W, McKinney K, Liu L, Lakhlani S, Jennes L. Distribution of vesicular glutamate transporter-2 messenger ribonucleic acid and protein in the septum-hypothalamus of the rat. Endocrinology 2003;144:662–670. [PubMed: 12538629]

Mai, JK.; Assheuer, J.; Paxinos, G. Atlas of the human brain. San Diego: Academic Press; 1997.

Martin RF, Bowden DM. A stereotaxic template atlas of the macaque brain for digital imaging and quantitative neuroanatomy. Neuroimage 1996;4:119–150. [PubMed: 9345504]

Palkovits M. Isolated removal of hypothalamic or other brain nuclei of the rat. Brain Res 1973;59:449–450. [PubMed: 4747772]

Palkovits M, Dobolyi A, Helfferich F, Usdin TB. Localization and chemical characterization of the audiogenic stress pathway. Annals of the New York Academy of Sciences 2004;1018:16–24. [PubMed: 15240348]

Palkovits M, Harvey-White J, Liu J, Kovacs ZS, Bobest M, Lovas G, Bago AG, Kunos G. Regional distribution and effects of postmortal delay on endocannabinoid content of the human brain. Neuroscience 2008;152:1032–1039. [PubMed: 18343585]

Paxinos, G.; Huang, X. Atlas of the human brainstem. Sydney: Academic Press; 1995.

Pfaff, DW.; Sakuma, Y.; Kow, LM.; Lee, AW.; Easton, A. Hormonal, Neural, and Genomic Mechanisms for Female Reproductive Behaviors, Motivation, and Arousal. In: Neill, JD., editor. Knobil and Neill's Physiology of Reproduction. Amsterdam: Academic Press; 2006. p. 1825-1920.

Stanic D, Brumovsky P, Fetissov S, Shuster S, Herzog H, Hokfelt T. Characterization of neuropeptide Y2 receptor protein expression in the mouse brain. I. Distribution in cell bodies and nerve terminals. J Comp Neurol 2006;499:357–390. [PubMed: 16998904]

Sugimura Y, Murase T, Ishizaki S, Tachikawa K, Arima H, Miura Y, Usdin TB, Oiso Y. Centrally administered tuberoinfundibular peptide of 39 residues inhibits arginine vasopressin release in conscious rats. Endocrinology 2003;144:2791–2796. [PubMed: 12810532]

Swann JM, Wang J, Govek EK. The MPN mag: introducing a critical area mediating pheromonal and hormonal regulation of male sexual behavior. Annals of the New York Academy of Sciences 2003;1007:199–210. [PubMed: 14993054]

Usdin TB. Evidence for a parathyroid hormone-2 receptor selective ligand in the hypothalamus. Endocrinology 1997;138:831–834. [PubMed: 9003022]

Usdin TB, Bonner TI, Hoare SR. The parathyroid hormone 2 (PTH2) receptor. Receptors Channels 2002;8:211–218. [PubMed: 12529938]

Usdin TB, Dobolyi A, Ueda H, Palkovits M. Emerging functions for tuberoinfundibular peptide of 39 residues. Trends Endocrinol Metab 2003;14:14–19. [PubMed: 12475607]

Usdin TB, Gruber C, Bonner TI. Identification and functional expression of a receptor selectively recognizing parathyroid hormone, the PTH2 receptor. J Biol Chem 1995;270:15455–15458. [PubMed: 7797535]

Usdin TB, Hilton J, Vertesi T, Harta G, Segre G, Mezey E. Distribution of the parathyroid hormone 2 receptor in rat: immunolocalization reveals expression by several endocrine cells. Endocrinology 1999a;140:3363–3371. [PubMed: 10385434]

Usdin TB, Hoare SR, Wang T, Mezey E, Kowalak JA. TIP39: a new neuropeptide and PTH2-receptor agonist from hypothalamus. Nat Neurosci 1999b;2:941–943. [PubMed: 10526330]

Usdin TB, Wang T, Hoare SR, Mezey E, Palkovits M. New members of the parathyroid hormone/parathyroid hormone receptor family: the parathyroid hormone 2 receptor and tuberoinfundibular peptide of 39 residues. Front Neuroendocrinol 2000;21:349–383. [PubMed: 11013069]

Varga T, Palkovits M, Usdin TB, Dobolyi A. The medial paralemniscal nucleus and its afferent neuronal connections in rat. J Comp Neurol 2008;511:221–237. [PubMed: 18770870]

Wang J, Coolen LM, Brown JL, Usdin TB. Neurons containing tuberoinfundibular peptide of 39 residues are activated following male sexual behavior. Neuropeptides 2006a;40:403–408. [PubMed: 17056109]

Wang J, Palkovits M, Usdin TB, Dobolyi A. Afferent connections of the subparafascicular area in rat. Neuroscience 2006b;138:197–220. [PubMed: 16361065]

Wang J, Palkovits M, Usdin TB, Dobolyi A. Forebrain projections of tuberoinfundibular peptide of 39 residues (TIP39)-containing subparafascicular neurons. Neuroscience 2006c;138:1245–1263. [PubMed: 16458435]

Wang T, Palkovits M, Rusnak M, Mezey E, Usdin TB. Distribution of parathyroid hormone-2 receptor-like immunoreactivity and messenger RNA in the rat nervous system. Neuroscience 2000;100:629–649. [PubMed: 11098126]

Ward HL, Small CJ, Murphy KG, Kennedy AR, Ghatei MA, Bloom SR. The actions of tuberoinfundibular peptide on the hypothalamo-pituitary axes. Endocrinology 2001;142:3451–3456. [PubMed: 11459790]

Wittmann G, Lechan RM, Liposits Z, Fekete C. Glutamatergic innervation of corticotropin-releasing hormone- and thyrotropin-releasing hormone-synthesizing neurons in the hypothalamic paraventricular nucleus of the rat. Brain Res 2005;1039:53–62. [PubMed: 15781046]

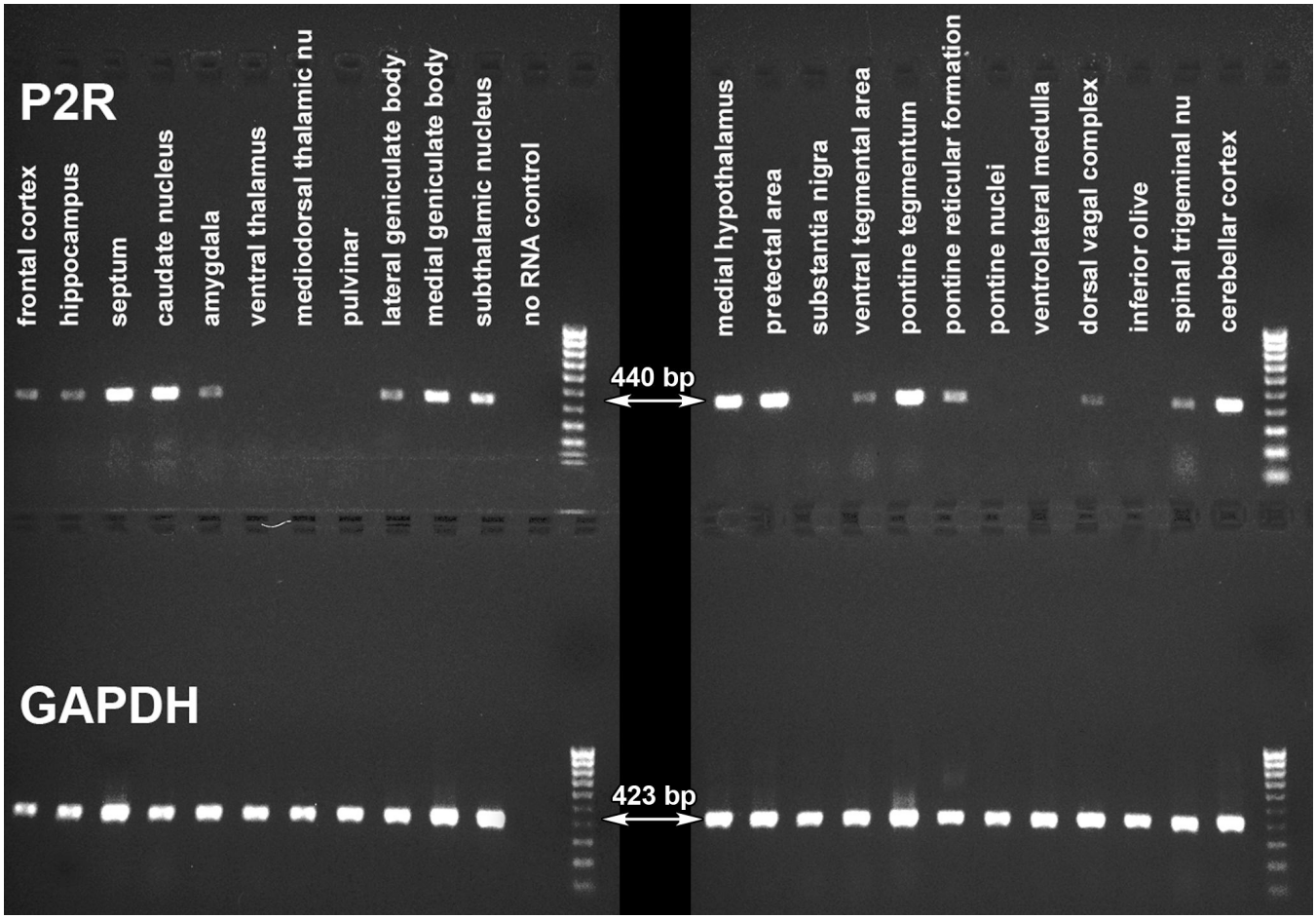

Fig. 1.

Expression of the PTH2R in the human brain detected by RT-PCR. Products of PCR reactions performed using cDNA templates from different human brain regions were run on gels. In the upper line, PTH2R-specific 440 bp PCR products are visible. The positive bands in several brain areas suggest a widespread expression of the PTH2R. In the lower line, bands of 423 bp from control PCR reactions performed using primers specific for the housekeeping gene GAPDH are present.

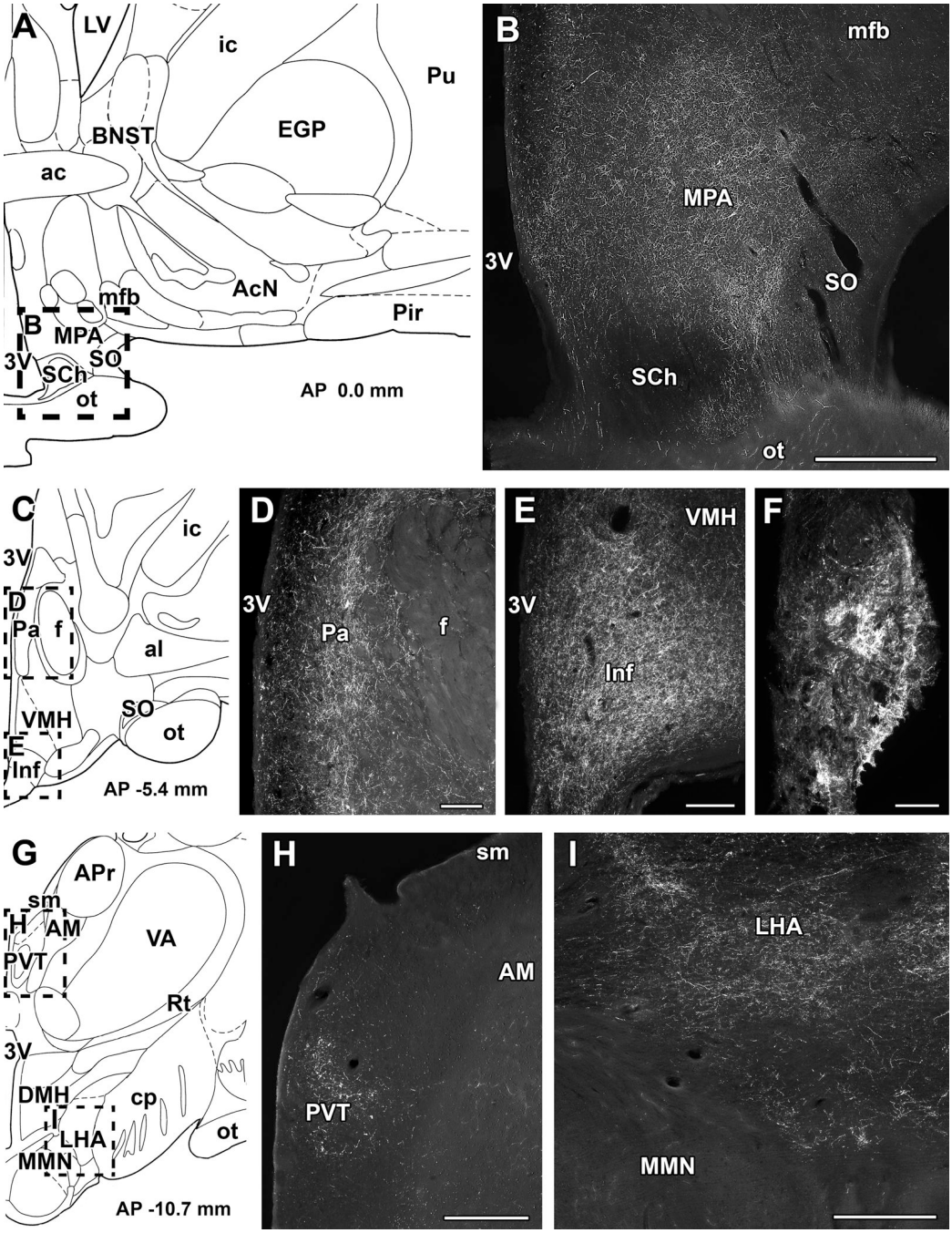

Fig. 2.

Immunolabeling of the PTH2R in the human diencephalon. Photomicrographs demonstrate PTH2R immunoreactivity visualized by FITC-tyramide fluorescent amplification immunocytochemistry. The presence of PTH2R-ir fibers is demonstrated in coronal sections of the human diencephalon. A - A schematic drawing shows a part of the human brain at the level of the preoptic area in the coronal plane. The framed area indicates the field in B. B - A dense network of PTH2R-ir fibers is present in the medial preoptic area. In contrast, the density of PTH2R-ir fibers is very low in the supraoptic nucleus, and PTH2R-ir fibers are absent in the suprachiasmatic nucleus. C - A schematic drawing shows a part of the human brain at the level of the paraventricular nucleus in the coronal plane. The framed areas correspond to fields

in D, and E, respectively. D - A high density of PTH2R-ir fibers is present in the hypothalamic paraventricular nucleus. E - The infundibular nucleus contains a high density of PTH2R-ir fibers. F - A very high level of PTH2R immunoreactivity is present in fiber terminals of the median eminence. G - A schematic drawing shows a part of the human brain at the level of the mamillary body in the coronal plane. H - PTH2R-ir fibers are abundant in the paraventricular thalamic nucleus but not in the adjacent anteromedial thalamic nucleus. I - The density of PTH2R-ir fibers is high in the lateral hypothalamic area. In contrast, PTH2R-ir fibers are absent from the medial mamillary nucleus. Schematic drawings (A, C, and G) are modifications from an atlas of the human brain (Mai et al., 1997). In agreement with the scaling of this atlas, antero-posterior coordinates (AP) are indicated from the level of the anterior commissure set as zero. Scale bars: 1 mm for B, H, and I, and 500 μm for D, E, and F.

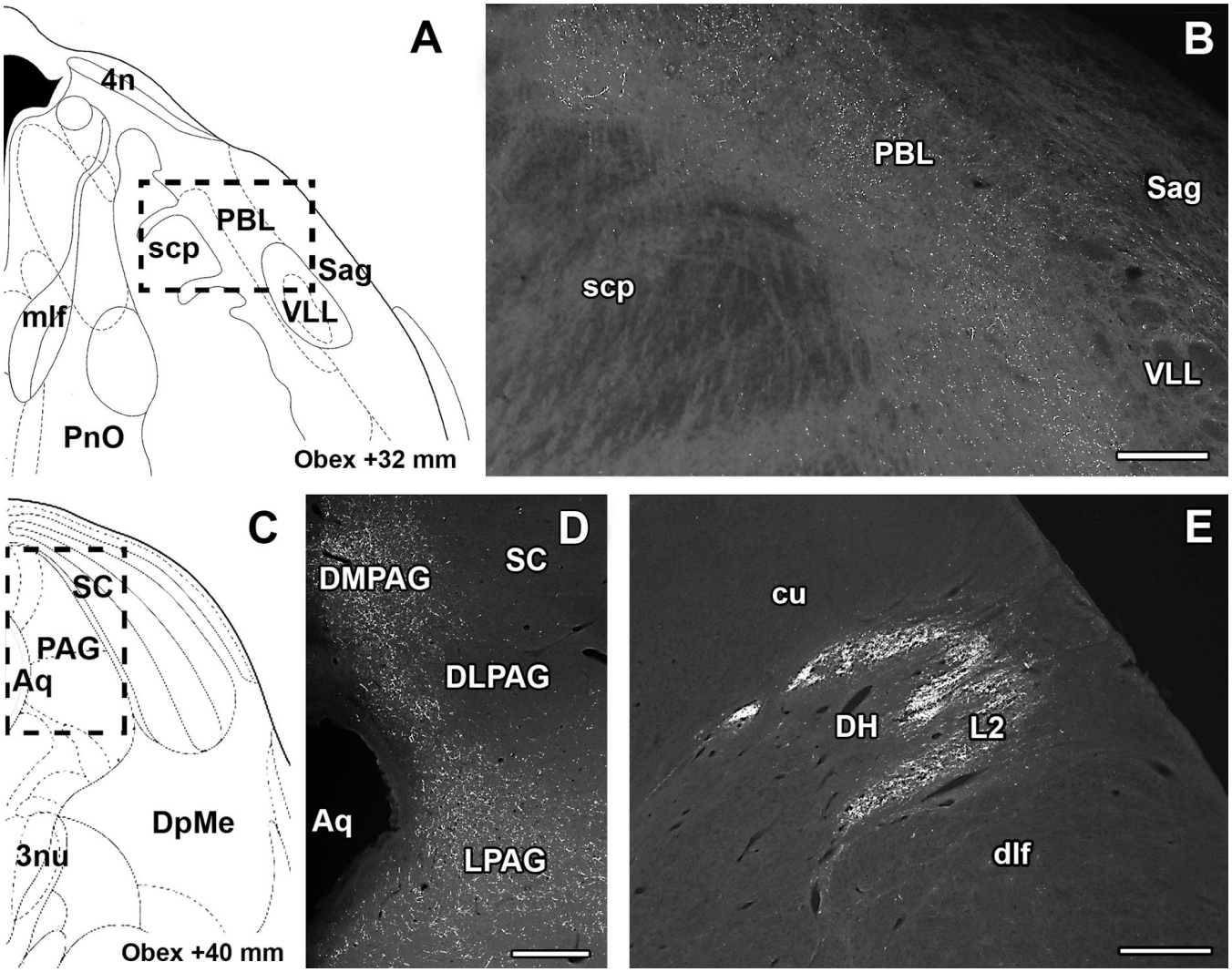

Fig. 3.

Immunolabeling of the PTH2R in the human brainstem and spinal cord. Photomicrographs demonstrate PTH2R immunoreactivity visualized by FITC-tyramide fluorescent amplification immunocytochemistry in coronal sections. A - A schematic drawing shows a section of the human pons in coronal plane. The framed area indicates the field in B. B - A high density of PTH2R-ir fibers is present in the lateral parabrachial nucleus whereas the adjacent sagulum nucleus and the ventral nucleus of the lateral lemnsicus do not contain PTH2R-ir fibers. C - A schematic drawing shows a mesencephalic section of the human brain in coronal plane. The framed area indicates the field in D. D - A dense network of PTH2R-ir fibers is present in the periaqueductal gray. A particularly high density of PTH2R-ir fibers is present in the dorsomedial and lateral subdivisions of the periaqueductal gray. E - A particularly dense network of PTH2R-ir fibers is present in lamina 2 of the dorsal horn as demonstrated at cervical segment 2. In contrast, the cuneate and dorsolateral fasciculi, and the deeper laminae of the dorsal horn do not contain more than few, sparse PTH2R-ir fibers. Schematic drawings (A and C) are modifications from an atlas of the human brainstem (Paxinos and Huang, 1995). Antero-posterior coordinates are indicated in agreement with the scaling of this atlas, with the level of the obex set as zero. Scale bars: 500 μm for B, D, and E.

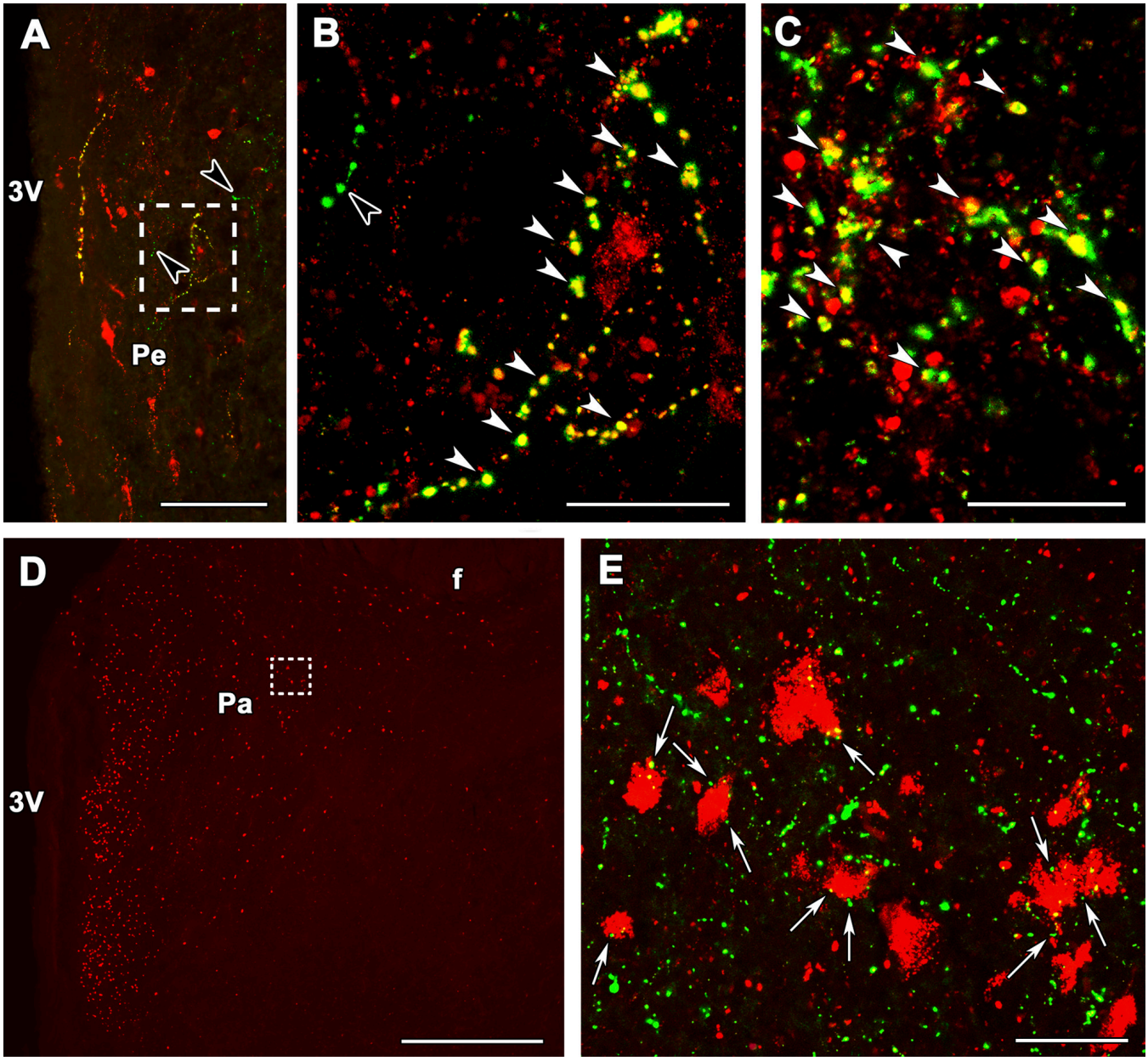

Fig. 4.

PTH2R-immunoreactive fibers in relation to somatostatin and CRH immunoreactivities in the human hypothalamic periventricular and paraventricular nuclei and in the median eminence. Photomicrographs demonstrate PTH2R-ir fibers in coronal sections labeled for somatostatin (A–C) and CRH (D–E). A - Somatostatin-ir cell bodies and fibers (red), PTH2R-ir fibers (green) indicated by black arrowheads, as well as double-labeled fibers (yellow) indicated by white arrowheads are present in the hypothalamic periventricular nucleus. The co-localization of somatostatin and the PTH2R suggests that a portion of somatostatin neurons contains PTH2R. B - The framed area in A is shown in a high magnification confocal image. C - Fibers containing only somatostatin immunoreactivity (red) as well as fibers, in which somatostatin and the PTH2R co-localize (yellow), are demonstrated in the median eminence in a high magnification confocal image. White arrowheads indicate some of the double-labeled fiber terminals. D - CRH-ir cell bodies and fibers are located in the hypothalamic paraventricular

nucleus. The framed area indicates the field in E. E - CRH-ir cell bodies and fibers (red) and PTH2R-ir fibers and fiber terminals (green) are shown in a high magnification confocal image. The lack of double-labeled yellow structures suggest no co-localization between CRH and the PTH2R. In turn, PTH2R-ir fiber terminals seem to closely appose CRH-ir cell bodies as indicated by white arrows. Scale bars: 200 μm for A, 50 μm for B, and E, 30 μm for C, and 1 mm for D.

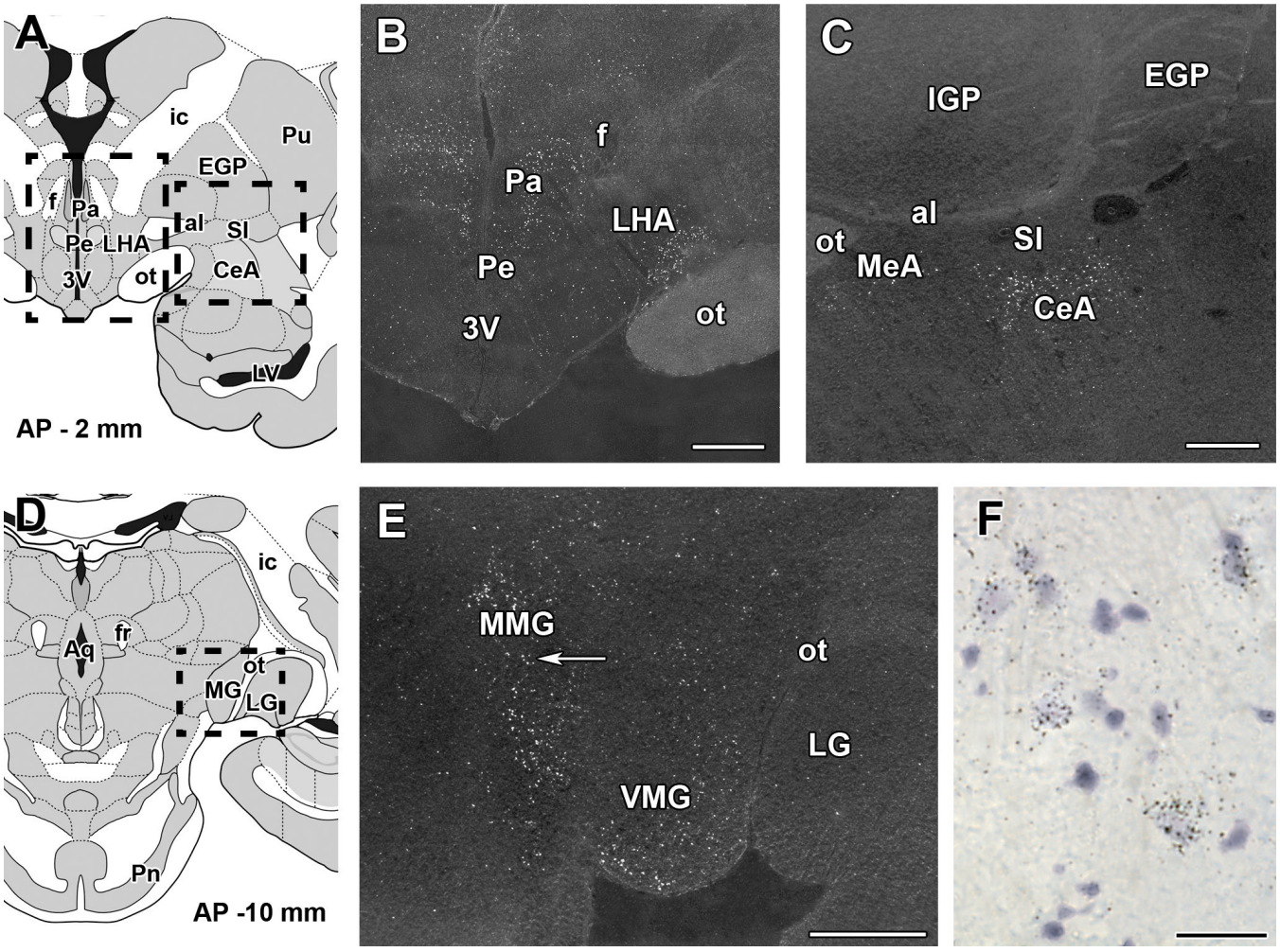

Fig. 5.

Expression of the PTH2R in diencephalic and amygdaloid regions of the macaque. The presence of mRNA encoding the PTH2R is shown by *in situ* hybridization histochemistry in coronal sections of the macaque brain. Positive autoradiography signals appear as white dots demonstrating the presence of TIP39 mRNA in the dark-field photomicrographs of emulsion dipped material. A - A schematic drawing shows a coronal section of the macaque brain through the hypothalamus and the amygdala. The framed areas indicate the fields in B and C. B - The dark-field photomicrograph shows a high density of PTH2R-expressing neurons in the hypothalamic paraventricular nucleus and in the ventral part of the lateral hypothalamic area. C - The dark-field photomicrograph shows a very high density of PTH2R-expressing neurons in the central amygdaloid nucleus and a lower density of PTH2R-expressing neurons in the medial amygdaloid nucleus. D - A schematic drawing shows a coronal section of the macaque brain at the level of the medial and lateral geniculate bodies. The framed area corresponds to the field in E. E - The dark-field photomicrograph shows a very high density of PTH2R-expressing neurons in the medial nucleus of the medial geniculate body while the PTH2R-expressing neurons are also abundant in the ventral nucleus of the medial geniculate body. In contrast, only few scattered PTH2R expressing cells are present in the lateral geniculate body. The arrow points to the field in F. F - A high magnification bright-field photomicrograph demonstrates the accumulation of individual autoradiography grains above cell bodies containing PTH2R mRNA in the medial geniculate body. Schematic drawings in all macaque

brain figures are modifications from an atlas of the macaque brain (Martin and Bowden, 1996), and antero-posterior coordinates (AP) are indicated in agreement with the scaling of this atlas, with the level of the anterior commissure set as zero. Scale bars: 1 mm for B, C, and E, and 30 μm for F.

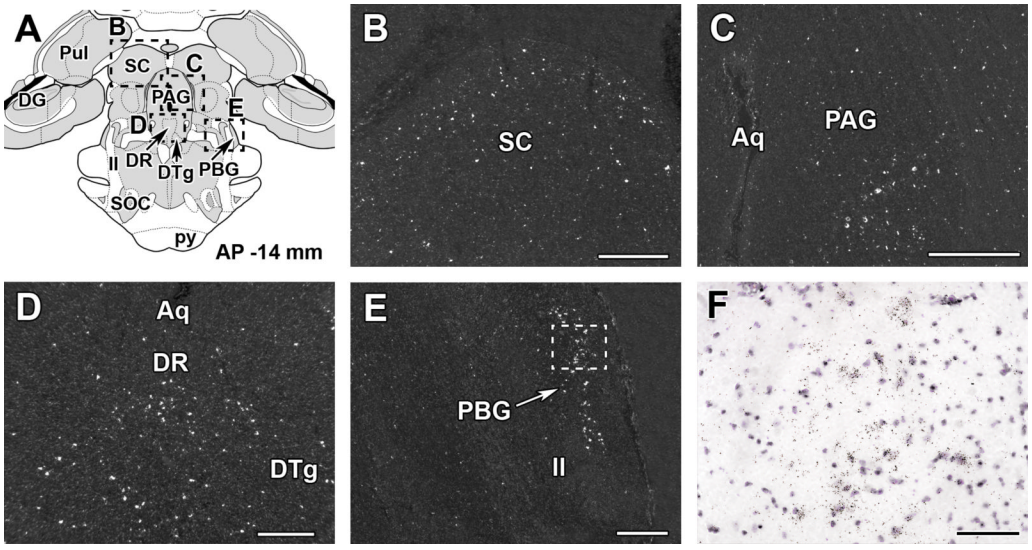

Fig. 6.

Expression of the PTH2R in the macaque midbrain. The presence of PTH2R encoding mRNA is exhibited by *in situ* hybridization histochemistry in coronal sections of the macaque midbrain. Positive autoradiography signals appear as white dots to demonstrate the presence of PTH2R mRNA in the dark-field photomicrographs. A - A schematic drawing shows a coronal section of the macaque midbrain. The framed areas indicate the fields in the dark-field photomicrographs in B-E. B - The dark-field photomicrograph shows that PTH2R-expressing neurons are abundant in the superior colliculus. The density of labeled neurons is especially high in the superficial layers. C -The dark-field photomicrograph shows PTH2R-expressing neurons in the periaqueductal gray. The density of labeled neurons is especially high in the ventrolateral subdivision. D - PTH2R-expressing neurons are abundant in the dorsal raphe nucleus. E - A high density of PTH2R-expressing neurons is present in the parabigeminal nucleus lateral to the lateral lemniscus. The framed area corresponds to the field in F. F - A high magnification bright-field photomicrograph demonstrates the accumulation of individual autoradiography grains above cell bodies containing PTH2R mRNA in the parabigeminal nucleus. Scale bars: 1 mm for B, and C, 500 μm for D, and E, and 100 μm for F.

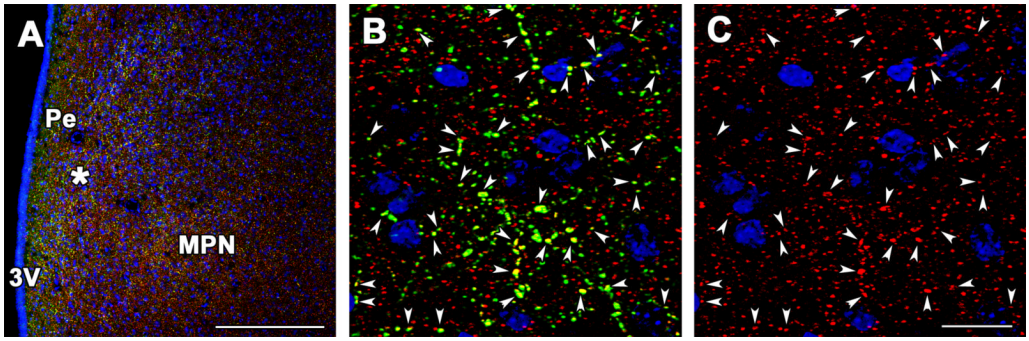

Fig. 7.

PTH2R-immunoreactive fibers, in relation to vesicular glutamate transporter 2 (VGLUT2)-immunoreactivity in a coronal section of the macaque medial preoptic area. A – A photomicrograph demonstrates that PTH2R-ir (green) fibers as well as VGLUT2 -ir (red) fibers and fiber terminals are present in the hypothalamic periventricular nucleus, the medial preoptic nucleus, and the adjacent preoptic regions. The nuclei of cell bodies are labeled blue with DAPI counterstaining. Star indicates the position of the field in B and C. B - The co-localization of PTH2R- and VGLUT2 -immunoreactivities (yellow) in the high magnification confocal image demonstrates that the majority of PTH2R-ir fiber terminals also co-localize VGluT2. Several of these double-labeled terminals are indicated by white arrowheads. In contrast, there are numerous VGluT2-containing fiber terminals that do not contain PTH2R as indicated by their red color. C - The same field as in B is shown without the green channel to demonstrate the presence of VGLUT2 immunoreactivity (red) in fiber terminals co-localizing PTH2R and VGLUT2 as indicated by white arrowheads. Scale bars: 300 μm for A, and 30 μm for B, and C.

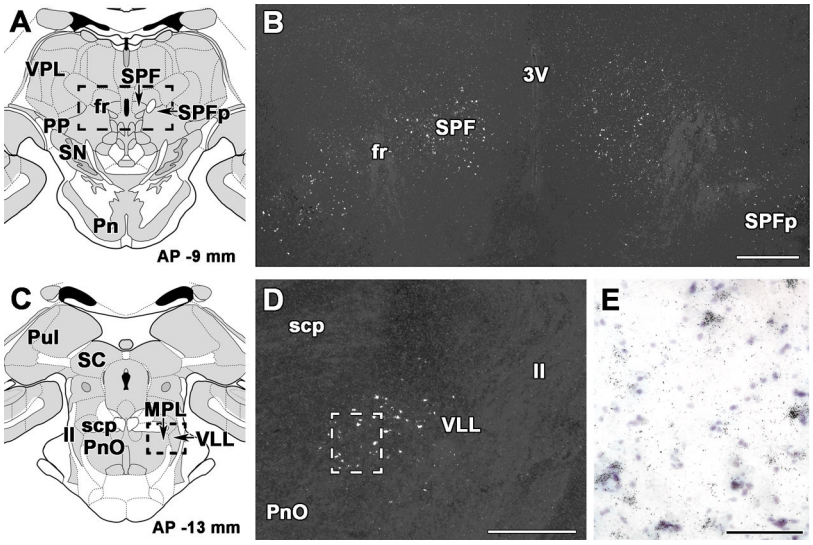

Fig. 8.

Expression of TIP39 in the macaque brain. The presence of mRNA encoding TIP39 is exhibited by *in situ* hybridization histochemistry in coronal sections of the macaque brain. Positive autoradiography signals appear as white dots to demonstrate the presence of TIP39 mRNA in the dark-field photomicrographs. A - A schematic drawing shows a coronal section of the macaque brain at the diencephalon-mesencephalon junction. The framed area indicates the field in B. B - The dark-field photomicrograph shows TIP39-expressing neurons located between the 3rd ventricle and the white matter of the fasciculus retroflexus in the subparafascicular area, as well as in the parvicellular subparafascicular nucleus lateral to the fasciculus retroflexus. C - A schematic drawing shows a coronal section of the macaque brain at the level of the ponto-mesencephalic junction. The framed area corresponds to the field in D. D - The dark-field photomicrograph shows TIP39-expressing neurons located in the medial paralemniscal nucleus immediately medial to the ventral nucleus of the lateral lemniscus. The framed area corresponds to the field in E. E - A high magnification bright-field photomicrograph demonstrates the accumulation of individual autoradiography grains above cell bodies containing TIP39 mRNA. Scale bars: 1 mm for B, and D, and 200 μm for E.

Table 1

Information on human tissue used in the study.

Brain Number	Gender	Age (years)	Clinical Diagnosis	Tissue	Detection method
1	female	89	Alzheimer disease	fresh frozen micropunched samples	RT-PCR
2	male	56	Cardiac failure	fresh frozen micropunched samples	RT-PCR
3	female	8	Leukemia	immersion fixed hypothalamus	immunolableling
4	male	10	Leukemia	immersion fixed insula, diencephalon, brainstem	immunolableling
5	male	62	Unknown	immersion fixed medulla and spinal cord (C1,2)	immunolableling

Table 2

Summary of the location of PTH2R mRNA and PTH2R-ir fibers in human and macaque, and their comparisons to mouse data.

Area	mRNA by RT-PCR in human	mRNA by ISHH in macaque	Cell bodies in mice	PTH2R-ir fibers in human	PTH2R-ir fibers in mice
Forebrain					
Cerebral cortex					
Frontal cortex	+		+		0
Insular cortex			++	+	+
Hippocampus	+	+	+		0
Septum	+++				
Medial septal nucleus			0		0
Lateral septal nucleus			+++		++
Amygdala	+				
Central nucleus		+++	++		++
Basal nuclei		+	+		0
Lateral nucleus		+	+		0
Medial nucleus		++	++		++
Cortical nucleus		+	+		+
Basal ganglia					
Caudate nucleus	+++	+	++		0
Putamen		0			
Globus pallidus		0	+		0
Claustrum			++		+
Nucleus accumbens			+		++
Substantia innominata		+	+		+
Diencephalon					
Thalamus					
Anterior thalamic nuclei		0	0	+	0
Midline thalamic nuclei		+	++	++	++
Lateral thalamic nuclei		0	0	+	+
Ventral thalamic nuclei	0	0	0	0	0
Reticular nucleus		0	0	0	0
Mediodorsal thalamic nucleus	0	0	0	0	0

Area	mRNA by RT-PCR in human	mRNA by ISHH in macaque	Cell bodies in mice	PTH2R-ir fibers in human	PTH2R-ir fibers in mice
Habenular nuclei		+	+	+	+
Posterior thalamic nuclei		0	0	+	+
Peripeduncular area		+	+	+	+
Suprageniculate thalamic nucleus		+	+	+	+
Medial geniculate body	+++				
dorsal nucleus		0	0	0	0
ventral nucleus		++	++	+	+
medial nucleus		+++	+++	++	++
Lateral geniculate body	+	+	+	+	+
Pulvinar	0	0			
Hypothalamus	+++				
Medial preoptic area		+++	+++	+++	+++
Lateral preoptic area		+	+	+	+
Supraoptic nucleus		+	+	++	++
Supraoptic decussations				++	++
Suprachiasmatic nucleus		0	0	0	0
Anterior hypothalamic nucleus		+	+	+	+
Paraventricular nucleus		+++	++	+++	+++
Periventricular nucleus		++	++	++	++
Arcuate (infundibular) nucleus		+	++	+++	+++
Median eminence				+++	+++
Ventromedial nucleus		+	+	+	+
Dorsomedial nucleus		+	+	++	++
Lateral hypothalamic area		++	+	++	++
Perifornical nucleus		+	+	+	+
Posterior hypothalamic nucleus		+	+	++	++
Tuberomamillary nucleus		+	+	++	++
Premamillary nuclei		+	+	++	++
Mamillary body					
Superior mamillary nucleus		+	++	+	++

Area	mRNA by RT-PCR in human	mRNA by ISHH in macaque	Cell bodies in mice	PTH2R-ir fibers in human	PTH2R-ir fibers in mice
Medial mamillary nucleus		0	0	0	0
Lateral mamillary nucleus		0	0	+	++
Subthalamic nucleus	++	+	+	+	+
Brainstem					
Midbrain					
Zona incerta		+	++	++	+++
Substantia nigra	0	0	0	0	0
Red nucleus		0	0	0	0
Subbrachial nucleus		+	+	++	++
Praetectal area	+++	+	+	++	++
Superior colliculus		+++	++	++	++
Inferior colliculus		+	+	++	++
Parabigeminal nucleus		+++			
Periaqueductal gray		++	++	+++	+++
Dorsal raphe nucleus		+++	++	++	+++
Ventral tegmental area	+	+	++	++	+++
Oculomotor nuclei		0	0	0	0
Pons					
Lateral lemniscal nuclei		0	0	0	0
Medial paralemniscal nucleus		0	0	+	+
Pontine tegmentum.	+++	++	++	++	++
Parabrachial nuclei		+	+		
medial				+	+
lateral				+++	+++
Pontine nuclei	0	0	0	0	0
Superior olive		0	0	+	+
Pontine reticular formation	+	+	0	+	+
Principal trigeminal nu.		+	+	++	++
Motor trigeminal nucleus		0	0	0	0
Pontine raphe nucleus		0	0	+	++

Area	mRNA by RT-PCR in human	mRNA by ISHH in macaque	Cell bodies in mice	PTH2R-ir fibers in human	PTH2R-ir fibers in mice
Vestibular nuclei		0	0	+	+
Medulla Oblongata					
Cochlear nuclei				0	0
Spinal trigeminal nucleus	+		+	+++	+++
Prepositus hypoglossal nucleus			0	0	0
Medullary reticular formation	0		0	+	+
Inferior olive	0		0	0	0
Dorsal vagal complex	+				
Nucleus of the solitary tract			++	++	++
Dorsal motor vagal nucleus			0	0	0
Area postrema			0	0	0
Motor hypoglossal nucleus			0	0	0
Nucleus ambiguus			0	0	0
Medullary raphe nuclei			0	0	0
Cerebellum					
Cortex	+++		++		+
Nuclei			0		0

The average number of labeled cells per section in the nucleus is none (0), 1–10 (+), 11–20 (++), or over 20 (+++). Similarly, the density of PTH2R-ir fibers and fiber terminals is represented as none to low (0), moderate (+), high (++), and very high (+++). The density of PTH2R immunolabeling in the hypothalamus and medulla oblongata is determined as the average of 2 brains. The mice data are based on our previous study (Faber et al., 2007).